Accepted Manuscript

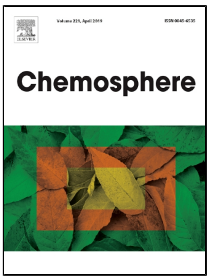

Neurotoxic assessment of Microcystin-LR, Cylindrospermopsin and their combination on the human neuroblastoma SH-SY5Y cell line

M.G. Hinojosa, A.I. Prieto, D. Gutiérrez-Praena, F.J. Moreno, A.M. Cameán, A. Jos

PII:	S0045-6535(19)30397-2
DOI:	10.1016/j.chemosphere.2019.02.173
Reference:	CHEM 23285
To appear in:	*Chemosphere*
Received Date:	29 October 2018
Accepted Date:	24 February 2019

Please cite this article as: M.G. Hinojosa, A.I. Prieto, D. Gutiérrez-Praena, F.J. Moreno, A.M. Cameán, A. Jos, Neurotoxic assessment of Microcystin-LR, Cylindrospermopsin and their combination on the human neuroblastoma SH-SY5Y cell line, *Chemosphere* (2019), doi: 10.1016/j.chemosphere.2019.02.173

Neurotoxic assessment of Microcystin-LR, Cylindrospermopsin and their combination on the human neuroblastoma SH-SY5Y cell line

Hinojosa MG[1], Prieto AI[1], Gutiérrez-Praena D[1*], Moreno FJ[2], Cameán AM[1], Jos A[1]

[1] Área de Toxicología, Facultad de Farmacia, Universidad de Sevilla, C/Profesor García González 2, 41012 Sevilla, Spain.

[2] Área de Biología Celular, Facultad de Biología, Universidad de Sevilla, Avda. Reina Mercedes s/n, 41012 Sevilla, Spain

* Corresponding author: Daniel Gutiérrez Praena. Área de Toxicología, Facultad de Farmacia, Universidad de Sevilla, C/Profesor García González 2, 41012 Sevilla, Spain. Mail: dgpraena@us.es

Abstract

Microcystin-LR (MC-LR) and Cylindrospermopsin (CYN) are produced by cyanobacteria. Although being considered as a hepatotoxin and a cytotoxin, respectively, different studies have revealed neurotoxic properties for both of them. The aim of the present work was to study their cytotoxic effects, alone and in combination, in the SH-SY5Y cell line. In addition, toxicity mechanisms such as oxidative stress and acetylcholinesterase (AChE) activity, and morphological studies were carried out. Results showed a cytotoxic response of the cells after their exposure to 0-100 μg/mL of MC-LR or 0-10 μg/mL CYN in both differentiated and undifferentiated cells. Thus, CYN resulted to be more toxic than MC-LR. Respect to their combination, a higher cytotoxic effect than the toxins alone in the case of undifferentiated cells, and almost a similar response to the presented by MC-LR in differentiated cells were observed. However, after analyzing this data with the isobolograms method, an antagonistic effect was mainly obtained. The oxidative stress study only showed an affectation of glutathione levels at the highest concentrations assayed of MC-LR and the combination in the undifferentiated cells. A significant increase in the AChE activity was observed after exposure to MC-LR in undifferentiated cells, and after exposure to the combination of both cyanotoxins on differentiated cells. However, CYN decreased the AChE activity only on differentiated cultures. Finally, the morphological study revealed different signs of cellular affectation, with apoptotic processes at all the concentrations assayed. Therefore, both cyanotoxins isolated and in combination, have demonstrated to cause neurotoxic effects in the SH-SY5Y cell line.

Keywords: MC-LR, CYN, MC-LR+CYN combination, SH-SY5Y cells, neurotoxicity

1. Introduction

Cyanobacteria are present in a variety of aquatic and terrestrial ecosystems due to their adaptive ability, even in extreme conditions (Svircev et al., 2014). Under favorable conditions of light, pH, nutrients (nitrogen and phosphorus) and interaction with other organisms, they present the capability of forming blooms and producing secondary metabolites called cyanotoxins, whose occurrence is increasing due to long term climate change (Buratti et al., 2017). According to their target organ, these toxins can be classified as hepatotoxins (e.g. microcystins, nodularins), dermatotoxins (e.g. lungbyatoxin), neurotoxins (e.g. anatoxin-a, homoanatoxin, saxitoxins), irritant toxins (e.g. lipopolysaccharides) and cytotoxins (e.g. cylindrospermopsin) (Testai et al., 2016). The exposure to these metabolites can occur by different paths such as the oral route, dermal contact or inhalation, although the oral route is the most significant one, since intoxication may take place by the intake of contaminated water, food or dietary supplements based on algae (Buratti et al., 2017). Among all cyanotoxins, microcystins (MCs) and cylindrospermopsin (CYN) have focused great interest, since they have been involved in the death of different animal species and humans (Azevedo et al., 2002; Bourke et al., 1983; Carmichael et al., 2001; Malbrouck and Kestemont, 2006).

Microcystins are cyclic heptapeptides synthetized by several cyanobacterial species such as *Mycrocistis aeruginosa, Oscillatoria agardhii, Plankthotrix agardii*, and *Planktothris rubescens,* etc. (Sivonen and Jones, 1999). Up to date, more than 246 congeners of MCs are known, being MC-LR the most potent congener and frequently identified (Spoof and Catherine, 2017). Mainly considered as a hepatotoxin, MC-LR can also affect other organs such as kidneys, heart or brain (Li et al., 2011; Qiu et al., 2009; Zeng et al., 2014, 2018). One of the main MC-LR-mechanisms of action is the inhibition of protein serine/threonine phosphatases, causing a cascade of effects such as

the deregulation of phosphoproteins, which lead to tumor promotion and apoptosis (MacKintosh et al., 1990). In addition, many studies have also demonstrated its *in vitro* cytotoxic potential in different cell lines from fish, mammals and humans (Ding et al., 2017; Feurstein et al., 2009; Gutiérrez-Praena et al., 2012; Meng et al., 2011, 2013; Pichardo et al., 2007; Rozman et al., 2017). Moreover, several authors have also described that this toxin induces oxidative stress by increasing reactive oxygen species (ROS) and reducing glutathione (GSH) levels, leading to cell apoptosis (Li et al., 2015; Liu et al., 2016; Puerto et al., 2011; Qian et al., 2018), although these effects have not been studied using human neuronal cell lines yet.

Cylindrospermopsin is an alkaloid consisting in a tricyclic guanidine combined to a hydroxylmethyl uracil group. This toxin presents a highly water-soluble structure, being commonly found out of the cells (Falconer and Humpage, 2006). Several cyanobaterial species are able to produce this toxin, such as *Cylindrospermopsis raciborskii*, *Umezakia natans*, *Chrysosporum ovalisporum, Anabaena bergii,* etc. (Banker et al., 1997; Harada et al., 1994; Schembri et al., 2001; Shaw et al., 1999). The main target of this cytotoxin is the liver, although kidneys, lungs, thymus, marrow bone, adrenal gland, gastrointestinal tract, immune, heart and nervous system have been also described as potential targets (Falconer et al., 1999; Guzmán-Guillén et al., 2015; Hawkins et al., 1985; Humpage et al., 2000; Terao et al., 1994). The most well-known mechanism of action of CYN is the inhibition of protein and GSH synthesis (Froscio et al., 2003; Runnegar et al., 1995; Terao et al., 1994). This cyanotoxin also enhances ROS production, which could lead to apoptosis or DNA damage (Gutiérrez-Praena et al., 2011, 2012; Guzmán-Guillén et al., 2013; Puerto et al., 2011). In addition, some studies have indicated the pro-genotoxic properties of CYN, being essential its previous

metabolic activation by the enzymatic cytochrome P-450 complex (CYP450) (Humpage et al., 2005; Puerto et al., 2018; Žegura et al., 2011).

Both cyanotoxins have evidenced to induce neurotoxic effects in different experimental models (Florzyck et al., 2014). Thus, MCs have shown to cause neuronal damage *in vitro* in different rodent cell lines such as primary murine cerebellar granule neurons (CGNs) and primary rat astrocytes (Feurstein et al., 2011; Rozman et al., 2017). Furthermore, many *in vivo* studies have manifested a clear neurotoxic potential, mostly of MC-LR, in different animal species such as rodents, fish and nematodes, affecting to their behavior, enhancing ROS levels, and modifying proteins related to neurodegenerative diseases (Baganz et al., 2004; Wang et al., 2013; Wu et al., 2017). In fact, MC-LR has produced pathological damage in hippocampus, neuronal degenerative changes, inflammation in memory-related brain regions and apoptosis in rats, suggesting that this toxin can be related to Alzheimer´s disease in humans (Li et al., 2012a; 2012b; 2014). Actually, some studies confirm its transport through the blood-brain-barrier using OATP1A2, a variant of the organic anion transport system (OATP), because of its relatively large hydrophilic structure (Feurstein et al., 2009; Fischer et al., 2005; Menezes et al., 2013). On the contrary, neurotoxic effects of CYN are still not well elucidated. In this sense, there is only one report studying its effects in different *in vitro* murine cell lines (Takser et al., 2016). Meanwhile, some *in vivo* reports have showed *in vivo* neurotoxic effects in snails, tadpoles and fish, such as behavioral alterations or histopathological changes (da Silva et al., 2018; Guzmán-Guillén et al., 2015; Kinnear et al., 2007; Kiss et al., 2002; White et al., 2007).

Moreover, it is worthy to point out that the majority of studies concerning cyanotoxins toxicity are focused on single purified toxins, setting apart the fact that organisms are exposed simultaneously to a wide variety of cyanotoxins when they are

present in aquatic systems. In fact, several studies have described the concomitant occurrence of MCs- and CYN-producing cyanobacteria, as well as the presence of both cyanotoxins at the same time (Bittencourt-Oliveira et al., 2014; Bogialli et al., 2006; Oehrle et al., 2010; Vasas et al., 2004). In the case of neurotoxicity, only a study conducted by Takser et al. (2016) showed the effects of a combination of MCs and CYN, although they also included the neurotoxin anatoxin-a in the combination (1:1:1).

The SH-SY5Y cell line is a commonly used neuronal model due to its biochemical and functional properties, being very appropriate for neurotoxicity studies. Moreover, the differentiation of this cell line provides functional, biochemical and morphologically mature neurons, which are more similar to those present in the human brain (Xie et al., 2010). For this reason, both types of SH-SY5Y cells are a very interesting experimental model to assess the possible damage induced by MC-LR and CYN in human neural cells.

Thus, considering all this, the aim of the present study was to assess the neurotoxic potential of MC-LR, CYN and their combination *in vitro* using the human neuroblastoma SH-SY5Y cell line, by exploring the cell viability, oxidative stress (ROS and GSH levels), acetylcholinesterase (AChE) activity and morphological changes after the exposure to these cyanotoxins.

2. Materials & Methods

2.1. Supplies and chemicals

MC-LR and CYN (both purity > 95% by HPLC) were purchased from Enzo Life Sciences. Minimum essential medium (MEM), cell culture reagents, and fetal bovine serum (FBS) were obtained from Gibco (Biomol, Sevilla, Spain). Nutrient Mixture F-12

Ham, retinoic acid (RA), and brain-derived neurotrophic factor human (BDNF) were purchased in Sigma-Aldrich (Madrid, Spain).

The MTS (3-(4,5- dimethylthiazol-2-yl)-5-(3-carboxymethoxyphenyl)-2-(4-sulphophenyl)-2H-tetrazolium salt) Cell Titer 96® AQueous One Solution Cell Proliferation Assay was purchased in Promega (Biotech Iberica, Madrid, Spain). The Bradford Reagent and the neutral red (NR) were purchased from Sigma-Aldrich (Madrid, Spain).

2.2. Model system

SH-SY5Y cells derived from a human neuroblastoma were obtained from ATCC (CRL-2266). They were maintained at 37˚C in an atmosphere containing 5% CO_2 at 95% relative humidity (CO_2 incubator, NuAire®, Spain) in a medium consisting in MEM and F-12 (1:1) supplemented with 10% FBS, 1% non-essential amino acids, 1% sodium piruvate, 1% L-glutamine 200 mM, and 1% penicillin/streptomycin solution. Cells were grown near confluence in 75-cm^2 plastic flasks and harvested weekly with 0.25% trypsin-EDTA (1X). Cells were quantified in a Neubauer chamber. SH-SY5Y cells were plated at density of $2 \cdot 10^5$ cells/mL to perform all the experiments.

2.3. Cell differentiation

SH-SY5Y cells were differentiated using the protocol provided by Encinas et al. (2000) with some modifications. Cells were plated at density of $5 \cdot 10^2$ cells/mL in plates of 48 wells, changing the medium every 48 hours with 1% of FBS, 10 µM RA and 50 ng/mL BDNF, for a week. The differentiation process was evaluated by morphological analysis.

2.4. Toxin test solutions

Stock solutions of 4 mg/mL MC-LR and 1 mg/mL CYN were prepared in absolute ethanol and sterilized milliQ water, respectively. Both solutions were maintained at -20˚C until their use.

2.5 Cytotoxicity assays

Undifferentiated SH-SY5Y cells were seeded in 96-well tissue-culture plates for basal cytotoxicity tests and incubated at 37˚C for 24 h prior to exposure. Differentiated cells were exposed after a week from the start of the differentiation process in the same 48-well plates where the differentiation process took place. From the stock solution of MC-LR, serial dilutions in medium without serum were prepared (20, 40, 60, 80, 100 µg/mL MC-LR). From the stock solution of CYN, serial dilutions in medium without serum were prepared (0.1, 0.2, 0.3, 0.4, 0.5, 0.75, 1, 2.5, 5, 10 µg/mL CYN). Vehicle control (ethanol) for MC-LR and a negative control (non-treated cells) were also included. After replacing the medium, exposure solutions were added to the plates, and incubated at 37°C for 24 and 48 h. The basal cytotoxicity endpoints assayed were protein content (PC), supravital dye neutral red cellular uptake (NR), and tetrazolium salt reduction (MTS). All the assays in the present paper were performed by triplicate.

Total protein content (PC) was quantified *in situ*, according to the procedure given by Bradford (1976), with modifications (Pichardo et al., 2007), in the same plates where exposure originally took place. The culture medium was replaced by 200 µL NaOH to dissolve the proteins and after 2 h of incubation at 37°C, 180 µL were replaced by the same volume of Bradford reagent. After 30-min incubation at room temperature, absorbance was read at 620 nm.

Neutral red uptake was performed according to Borenfreund and Puerner (1984) in the undifferentiated cells. The culture medium was replaced by 100 µL modified

192 medium without serum containing 10 mg/mL NR. The plate with the NR-containing
193 medium was returned to the incubator for another 3 h to allow the uptake of NR into the
194 lysosomes of viable cells. Thereafter, medium was removed, and cells were fixed for
195 2 min with a formaldehyde–$CaCl_2$ solution. By adding 200 µL of acetic acid–ethanol
196 solution to the wells, NR absorbed by cells was extracted, solubilized, and quantified at
197 540 nm.

198 The MTS reduction was measured according to Baltrop et al. (1991) in both
199 undifferentiated and differentiated cells. The MTS (3-(4,5-dimethylthiazol-2-yl)-5-(3-
200 carboxymethoxyphenyl)-2-(4-sulfophenyl)-2H-tetrazolium salt) tetrazolium compound
201 was added to the medium and, by bioreduction of cells, produces a colored formazan
202 product soluble in culture medium, which is immediately measured at 490 nm after 3 h
203 of incubation in the dark.

204 *2.6. Assessment of the effect of cyanotoxins combination by the isobolograms method*

205 Concentrations used to evaluate the toxic potential of the combination MC-LR -
206 CYN were selected based on the cytotoxicity results of the single cyanotoxins
207 previously obtained in both types of SH-SY5Y cells. The mean effective concentration
208 (EC_{50}) values obtained for the most sensitive endpoint at 24 h were chosen as the
209 highest exposure concentrations for the combination studies, along with the fractions
210 $EC_{50}/2$ and $EC_{50}/4$. Thus, SH-SY5Y cells were exposed for 24 and 48h to binary pure
211 cyanotoxins combinations: EC_{50} MC-LR + EC_{50} CYN, $EC_{50}/2$ MC-LR + $EC_{50}/2$ CYN
212 and $EC_{50}/4$ MC-LR + $EC_{50}/4$ CYN, and the MTS reduction assay was performed.
213 Moreover, each concentration used in the combinations was evaluated for each
214 individual cyanotoxin, also using the MTS assay.

The isobologram method was used to determine the type of interaction that occurs when MC-LR and CYN are in combination in undifferentiated and differentiated SH-SY5Y cells. This method was carried out according to Tatay et al. (2014). The isobologram analysis involves plotting the concentration-effect curves for each compound and its combinations in multiple diluted concentrations by using the median-effect equation, as described by Chou and Talalay (1984) and Chou (2006). These authors introduced the term of combination index (CI) for the quantification of synergism, additivity or antagonism of two compounds. When the CI < 1, indicates synergism, when CI is =1, indicates additivity, and when CI is >1, indicates antagonism. The CI_{50}, CI_{75} and CI_{90} are the concentrations required to inhibit proliferation at 50%, 75% and 90%, respectively. The CalcuSyn software (version 2.1) calculated these CI values automatically (Biosoft, Cambridge, UK, 1996–2007). The type of interaction produced by MC-LR and CYN combinations was assessed by an isobologram analysis using the same software. The parameters *Dm*, *m*, and *r* of the combinations, are the antilog of x-intercept, the slope and the linear correlation coefficient of the median-effect plot, respectively, and they give information about the shape of the concentration–effect curve.

2.7. Oxidative stress assays

2.7.1. Reactive Oxygen Species (ROS) generation

The production of ROS was assessed in 96-well plates using the dichlorofluorescein (DCF) assay (Puerto et al., 2010) in undifferentiated cells. Cells were incubated with 200 µL 40 µM DCF in the culture medium at 37˚C for 30 min. Then, cells were washed with PBS and exposed to the different concentrations of the toxins, according to the cytotoxicity results previously obtained (0-37 µg/mL MC-LR

239 and 0-1 µg/mL CYN). A solution of 200 µM $MnCl_2 \cdot 4H_2O$ was used as a positive
240 control. The plates were incubated for 4, 8, 12 and 24 h. Fluorescence was measured at
241 535 nm (emission) and 485 nm (excitation).

242 *2.7.2. Glutathione (GSH) content*

243 Glutathione (GSH) content was evaluated by reaction with the fluorescent probe
244 monochlorobimane (mBCL) (Jos et al., 2009) in undifferentiated cells. Cells were
245 exposed to the toxins (0-37 µg/mL MC-LR and 0-1 µg/mL CYN), according to the
246 previous results obtained in the cytotoxicity assays and incubated for 4, 8, 12 or 24 h. A
247 solution of 1 µM buthionine sulfoximine (BSO), a GSH synthesis inhibitor, was used as
248 positive control. After the exposure time, medium was discarded and cells were
249 incubated for 20 min at 37˚C in the presence of 40 µM mBCL. After that, cells were
250 washed with PBS and the fluorescence was measured 460 nm (emission) and 380 nm
251 (excitation).

252 *2.8. Acetylcholinesterase (AChE) activity determination*

253 Acetylcholinesterase activity was measured according to the method described
254 by Ellman et al. (1961) with modifications of Santillo et al (2015) in both
255 undifferentiated and differentiated cells. Viable SH-SY5Y cells were exposed to the
256 toxins, according to the previous results provided by the cytotoxicity assays (0-37
257 µg/mL MC-LR and 0-1 µg/mL CYN in undifferentiated cells; 0-45 µg/mL MC-LR and
258 0-0.3 µg/mL in differentiated cells) and incubated for 24 h at 37˚C. A solution of 50 nM
259 parathion was used as positive control. Afterwards, 200 µL of a reaction mixture
260 containing 0.5 mM 5,5-dithio-bis-(2-nitrobenzoic acid) (DTNB) and 100 µM
261 acetyltiocholine (ATCh) were added to each well. The resulting product of the reaction,
262 5-thio-2-nitrobenzoate (TNB), was measured at 410 nm every 90 s up to 60 min.

263 *2.9. Morphology*

264 The concentrations used for the morphological assay were the previously
265 calculated EC_{50} (24h) values. These values were chosen as the highest exposure
266 concentration along with the fractions $EC_{50}/2$ and $EC_{50}/4$. Undifferentiated and
267 differentiated SH-SY5Y cells were exposed for 24 h. Afterwards, cells were directly
268 fixed with a 1.6% glutaraldehyde in 0.1 M cacodylate buffer solution (pH 7.2) for 60
269 min at 4ºC. Later, they all were postfixed in 1% osmium tetroxide during the same time
270 and temperature. Time elapsed, samples were dehydrated in ethanol at progressively
271 higher concentrations and embedded in epoxy embedding medium (Epon). Toluidine
272 blue-stained semi-thin sections (0.5 mm thick) used as controls were viewed in a Leit
273 (Aristoplan) light microscope. Thin sections (60-80 nm thick) were cut on a Reichert-
274 Jung Ultracut E ultramicrotome, stained with uranyl acetate and lead citrate, and
275 examined in a Philips CM-10 transmission electron microscope. Cell growth and
276 development of morphology damage was observed using a Leica DMIL inverted
277 microscope by phase contrast.

278 *2.10. Calculations and statistical analysis*

279 Data for the cytotoxicity assays and oxidative stress biomarkers were presented
280 as mean ± standard deviation (SD) in relation to control. Statistical analysis was carried
281 out using analysis of variance (ANOVA), followed by Dunnett's multiple comparison
282 tests using GraphPad InStat software (GraphPad Software Inc., La Jolla, USA).
283 Differences were considered significant from $P<0.05$. EC_{50} values were derived by
284 linear regression in the concentration-response curves.

285 **3. Results**

286 *3.1. Cytotoxicity assays*

A concentration dependent decrease of both undifferentiated and differentiated SH-SY5Y cells viability was observed after their exposure to 1-100 µg/mL MC-LR at 24 and 48 h (Fig. 1). The EC_{50} values obtained in all the cytotoxicity assays performed are shown in Table 1. In the case of both differentiated and undifferentiated cells, MTS assay demonstrated to be the most sensitive biomarker, providing lower EC_{50} values in undifferentiated cells after the exposure times considered, compared to the differentiated cultures (Table 1).

Regarding to CYN, a concentration dependent decrease of viability was observed as well (Fig. 2). Using the MTS assay as a reference for its sensitivity, a higher cytotoxic response could be appreciated after 24 hours of exposure in differentiated cells compared to the undifferentiated, that response is contrary to that obtained after 48 hours of exposure (Table 1).

The concentration-response curves of the two cyanotoxins combination after the MTS assay, which demonstrated to be the most sensitive biomarker for both toxins in both types of cells, are shown in figure 3. The toxin combination proved to be more cytotoxic at the highest concentration tested on undifferentiated cells compared to the individual cyanotoxins after both exposure periods. On the contrary, on differentiated cells the response of the toxins combination was similar to the observed for MC-LR.

3.2. Assessment of the effect of cyanotoxins combination by the isobolograms method

In the experiment performed with undifferentiated cells, the cyanotoxin combination presented a CI > 1, which confirmed an antagonistic mode of action between these two toxins on SH-SY5Y cells (Table 2 and Fig. 4A, B). Data in Table 2 demonstrate that CI values were from antagonism (CI = 1.60-1.10) to moderate (CI = 1.45-1.08) effect over a wide range of EC_{50}-EC_{90} concentrations of MC-LR and CYN in

311 combination. The strongest antagonistic effect was observed after 48 h. Moreover, this
312 effect was more pronounced at lower concentrations.

313 In the experiment performed with the differentiated cells, the cyanotoxin
314 combination presented a CI > 1, confirming again an antagonistic mode of action
315 between these two toxins on differentiated SH-SY5Y cells (Table 3 and Fig. 4C, D).
316 Data in Table 3 demonstrate that CI values were equivalent to an antagonistic effect (CI
317 = 2.08-1.65) over the range of EC_{50}-EC_{90} concentrations of MC-LR and CYN in
318 combination. The strongest antagonistic effect was observed after 24 h.

319 *3.3. Oxidative stress assays*

320 The exposure to 9.25, 18.5 or 37 µg/mL MC-LR leaded to no significant
321 changes in the ROS assay in SH-SY5Y cells after 4, 8, 12 or 24 h of exposure.
322 However, it showed significant differences after 24 h of exposure to all the
323 concentrations tested in the GSH assay, and after 12 h of exposure to the highest
324 concentration (Fig. 5).

325 After exposure to 0.25, 0.5 or 1 µg/mL CYN, no significant differences were
326 observed in any of the exposure times assayed in either of the oxidative stress
327 biomarkers evaluated (Fig. 6) compared to the control group.

328 Similarly to the cell behavior after toxins exposure individually, SH-SY5Y did
329 not produced any significant difference in the ROS assay after the exposure to MC-LR+
330 CYN combination, but it did after 4 h of exposure to the highest concentration, and after
331 8 h in the other two concentrations in the GSH assay (Fig. 7).

332 *3.4. Acetylcholinesterase (AChE) activity*

A significant increase of AChE activity on undifferentiated SH-SY5Y cells was observed only after the highest concentration of MC-LR assayed (37 µg/mL). However, neither CYN nor its combination with MC-LR induced significant changes in this enzymatic activity (Fig. 8A).

In the case of the differentiated cells, a significant decrease of AChE activity was shown after exposure to all CYN-concentrations assayed (0.075-0.3 µg/mL). Nevertheless, although MC-LR did not produce significant changes, exposure to the mixture at the highest concentrations (45 and 0.3 µg/mL of MC-LR and CYN, respectively) led to an increase in this enzymatic activity (Fig. 8B).

3.5. Morphology study

Unexposed undifferentiated SH-SY5Y cells observed under phase-contrast microscope showed scarce cytoplasmic projections, frequently two of them placed in opposite directions. These projections usually present connections with nearby cells (Fig. 9A). The light microscope revealed mitotic cells with big nuclei and nucleoli (Fig. 9B). Under electronic microscope, cells present irregular nuclei with heterochromatin condensation and big nucleoli. In the cytoplasm stand out a big number of free ribosomes, mitochondria were scarce and presented dense matrix (Fig. 9C). In the non-treated differentiated cells, a high number of cytoplasmic projections was observed under the phase-contrast microscope (Fig. 10A). Under light microscopy, cells presented a fusiform shape with endoplasmic reticulum dilatations and lipidic vacuoles (Fig. 10B). The electron microscope revealed a cell cytoplasm with a higher number of microtubules and intermediate filaments than the undifferentiated cells (Fig. 10C).

3.5.1. Microscope observations of cells exposed to pure MC-LR

Undifferentiated cells exposed to 37 µg/mL MC-LR presented, under phase-contrast, light and electronic microcopies, cell death signs, with a reduction of their size, chromatin condensation, and numerous vacuoles in the cytoplasm in fragmentation process. Moreover, apoptotic nuclei with chromatin and nucleolar segregation were observed (Fig. 11A-D). At the lowest concentrations (18.5 and 9.25 µg/mL MC-LR), the most characteristic observations under phase-contrast microscope were the cytoplasmic projections by way of lamellipodium (Fig. 11E). The light microscope revealed cellular cycle arrest in the mitosis phase and nuclei with irregular shape and big nucleoli (Fig. 11F). Under the TEM, cells presented chromatin condensation in the nuclear membrane, segregated nucleoli and formation of autophagosomes (Figs. 11G and H).

Differentiated SH-SY5Y cells exposed to 45 µg/mL MC-LR showed an elevated refringence under the phase-contrast microscope caused by numerous dead cells and apoptotic bodies, as it could also be observed by light microscopy (Fig. 12A-B). Under electron microscopy, the presence of a large quantity of confluent heterophagosomes, nucleolar segregation, and numerous lipidic vacuoles were observed (Fig. 12C-D). At the lowest concentrations assayed (22.5 and 11.25 µg/mL MC-LR), cells observed under phase-contrast, light and electronic microcopies presented protein granules, possibly caused by alterations in the protein folding, lipidic vacuoles and chromatin condensation. Mitotic processes were also observed, although this phenomenon could be stopped due to the adverse situation induced by MC-LR (Fig. 12E-J).

3.5.2. Microscope observations of cells exposed to pure CYN

At the highest concentration assayed (1 µg/mL), undifferentiated cell cultures presented clear morphological alterations leading to cell death such as apoptotic bodies,

and heterochromatin condensation (Fig. 13A and B). Ultrastructurally, nuclei presented irregular shape and, frequently, the presence of apoptotic nuclei is high, with cytoplasmic fragmentation. In addition, segregated nucleolus was observed, being only visible their fibrillar component (Fig. 13C). At 0.5 and 0.25 µg/mL CYN, no remarkable morphological alterations were observed under light microscopy, where it is possible to observe the cellular cycle in mitosis phase. The TEM showed euchromatic nuclei and numerous mitochondria in the cytoplasm, a characteristic of undifferentiated cells (Fig. 13D and E).

After differentiation, SH-SY5Y cells exposed to the highest CYN concentration (0.3 µg/mL CYN) experienced a massive cell death, easily observable by phase-contrast (high refraction) and light (many cellular debris) microscopies. No cell division was observed (Fig. 14A-B). Ultrastructurally, apoptotic nuclei with heterochromatin condensation were appreciated, together with the presence of heterophagosomes (Fig. 14C). After exposure to 0.15 and 0.075 µg/mL CYN, cells presented an increased number of ribosomes compared to control cells. Moreover, an increment in lipidic vacuoles and dilated endoplasmic reticuli was observed. Nuclei presented the typical apoptotic morphology (Fig. 14D-I).

3.5.3. Microscope observations of cells exposed to the combination MC-LR/ CYN

Concerning the combinations, the combination with the highest CYN and MC-LR concentrations (1 + 37 µg/mL) induced and intense cell death in undifferentiated cells, mainly by apoptosis, appearing numerous cellular debris and apoptotic bodies. Moreover, apoptotic nuclei with chromatin condensation were observed (Fig. 15A and B). The combination composed by 0.5 + 18.5 µg/mL induced a moderate cell death by

403 apoptosis, were cells presented blisters in the surface, a typical observation in cells
404 dying by apoptosis (Fig. 15C and D).

405 Differentiated cells presented two extremes. At the highest concentration
406 assayed (0.3 + 45 μg/mL CYN + MC-LR), a remarkable cell death was observed, with
407 the presence of pre-apoptotic bodies all over the culture. On the other hand, when cells
408 were exposed to the other two concentrations, zones without any visible damage and
409 zones with intense cellular death were perceived (Fig. 16A-C). The TEM showed
410 numerous indicators of cellular damage in cells exposed to the highest exposure
411 concentration. Thus, lipidic degeneration, apoptotic nuclei, endoplasmic reticulum with
412 protein concentration, pre-apoptotic bodies, heterophagosomes, nuclear bodies, and
413 nucleolar segregation were observed (Fig. 16D-G).

414 **4. Discussion**

415 Microcystin-LR and CYN have been extensively studied *in vitro* in hepatic and
416 renal cell lines (Chen and Xie, 2016; McLellan and Manderville, 2017; Pichardo et al.,
417 2017). However, the studies concerning neuronal cell lines are still scarce, although
418 some *in vivo* studies point out that these cyanotoxins could induce neurotoxic effects
419 (Guzmán-Guillén et al., 2015; Kist et al., 2012; Qian et al., 2018; Wu et al., 2016;
420 2017). Neurotoxicity of cyanotoxins has been reviewed, including the main mechanisms
421 and effects (Florczyk et al., 2014; Hu et al., 2016) although the molecular mechanisms
422 underlying these effects have not been still elucidated yet. In this sense, the present
423 work focused on the potential effects induced by MC-LR, CYN, and their combination
424 in the human neuronal SH-SY5Y cell line. For MC-LR, only Zhang et al. (2018) used
425 this experimental model but for different purposes, such as transport, bioaccumulation,
426 hyperphosphorylation of PP2A-dependent Tau sites, and cell death. In the case of CYN

427 and its combination with MC-LR, the present study shows their effects *in vitro*,
428 contributing to mend the lack of information about this matter.

429 Regarding to MC-LR, our results showed a decrease of the cell viability after 24
430 and 48 h of exposure to MC-LR in both undifferentiated and differentiated cells, being
431 the undifferentiated the most sensitive cells. According to our results, several authors
432 have described a reduction of cell viability in different neuronal cell lines exposed to
433 MC-LR (primary murine WBC, primary murine CGNs cells, primary hippocampal
434 neurons, RAW246.7 murine macrophage-like cells, BV-2 cells, N2a cells, GT1-7 cells
435 and SH-SY5Y cells) (Cai et al., 2015; Ding et al., 2017; Feurstein et al., 2009; 2011; Li
436 et al., 2015; Takser et al., 2016; Zhang et al., 2018). However, most of these authors
437 used MC-LR concentrations up to 10 μM for 24, 48 or 72 h of exposure, and although
438 they described decreases in cell viability, only Cai et al. (2015) referred an EC_{50} value
439 for pure MC-LR. These authors exposed cells up to 30 μM MC-LR, establishing an
440 EC_{50} of 10 μM MC-LR in primary hippocampal neurons after 24 h of exposure using
441 the MTT cytotoxicity assay. In this regard, the presence of organic anion transporting
442 polypeptide transporters (OATPs) has been described as an important requirement to
443 MC-LR toxicity. It is well known that the OATP1B subfamily members are MCs
444 transporters (Fischer et al., 2005). Fischer et al. (2005) suggested that OATP1A2
445 transporters expressed in brain capillary endothelial cells and in the cell membrane of
446 human neurons could be involved in MC-LR transport through the blood-brain barrier.
447 In addition, Ding et al. (2017) demonstrated the role of the Oatp1a5 transporting MC-
448 LR into neuronal cells. These facts support that MC-LR damage could only evolve if it
449 is transported into the nervous system through OATPs or other different transporters
450 (Feurstein et al., 2009; 2011). However, the presence of these transporters in the
451 nervous system is scarce and, in some cases, their number can vary with the

452 differentiation process (Rozman et al., 2017; Yagdiran et al., 2016). Thus, the low MC-
453 LR-toxicity in those cell lines (primary murine WBC, primary murine CGNs cells,
454 primary hippocampal neurons, RAW246.7 murine macrophage-like cells, BV-2 cells,
455 N2a cells, GT1-7 cells and SH-SY5Y cells) and the increment in the EC_{50} value in the
456 differentiated SH-SY5Y cells from our study, compared with the undifferentiated ones,
457 could be due to this fact.

458 The potential mechanisms by which MC-LR induces its neurotoxic effects
459 include effects on neurotransmitters, neurochannels, signal transduction, oxidative stress
460 and cytoskeleton disruption (Hu et al., 2016). The neurotoxicity of MCs seems a multi-
461 pathway process, although the molecular mechanisms remain evasive. In this sense, Cai
462 et al. (2015) described that MC-LR disrupt calcium homeostasis in neurons, inducing a
463 concentration-dependent increment of intracellular free Ca^{2+} levels from stores together
464 with a decrease in cell viability. In agreement with these findings, Li et al. (2015)
465 reported that increased intracellular Ca^{2+} levels led to an activation of the phosphatase
466 calcineurin, which result in apoptosis via dephosphorylation of the proapoptotic Bcl-2
467 family member Bad. This calcium release, together with the associated cytochrome C
468 release, also activates the caspases protein family, well-known apoptotic proteins. Thus,
469 Feurstein et al. (2011) and Rozman et al. (2017) demonstrated that MC-LR induced cell
470 death by apoptosis through the activation of caspase proteins in primary murine CGN
471 cells and primary rat astrocytes, respectively. These findings support our results, since
472 our most sensitive cytotoxicity biomarker was the MTS assay, which assesses the
473 mitochondrial health and its activity, which is related with cell death (Tait and Green,
474 2013). Zhang et al. (2018) demonstrated that 10 μM MC-LR with endoporter caused
475 cell death in SH-SY5Y cells by using the lactate dehydrogenase (LDH) release assay. In
476 this experimental model, the authors indicated that MC-LR induced phosphorylation of

477 protein Tau, promoting dissociation of Tau from microtubules and aggregation of
478 phospho-paired helical filaments-Tau, and consequently, neuronal degeneration and cell
479 death. Cytoskeleton disruption is considered to be one of the cytotoxicity triggering
480 caused by MC-LR (Hu et al., 2016) based on the alterations induced *in vivo* by the toxin
481 in diverse cytosqueletal proteins in brains of rats (Zhao et al., 2015), and in *in vitro*
482 experiments (Meng et al., 2011).

483 Cellular death can be also corroborated through morphological studies. In this
484 regard, the present work shows how MC-LR induced the most common characteristics
485 of cellular death such as cytoplasm fragmentation, chromatin condensation, and
486 nucleolar segregation, endoplasmic reticulum dilatation, lipidic vacuoles, and presence
487 of heterophagosomes, both in the undifferentiated and differentiated SH-SY5Y cells. In
488 this sense, Feurstein et al. (2011) found that MC-LR induced a slight impairment of the
489 neurite network in primary murine CGN cells. In addition, Meng et al. (2011) described
490 some apoptotic effects such as the reorganization of cytoskeletal architectures in
491 differentiated PC12 cells exposed to 10 μM MC-LR, which was also observable in the
492 differentiated SH-SY5Y cells from our study. Moreover, Zhang et al. (2018) described
493 neurites degeneration and cell death in SH-SY5Y cells exposed to 10 μM MC-LR.

494 Two other toxic mechanisms studied in the present work are the oxidative stress
495 generation and the AChE disruption. For the oxidative stress evaluation two related
496 parameters were studied, ROS generation and GSH depletion, since it has been stated
497 that free-radical damage is one of the toxic mechanisms of MC-LR (Meng et al., 2013).
498 In the present work, ROS levels did not suffer any alteration in undifferentiated cells
499 exposed to pure MC-LR. However, Meng et al. (2013) found that concentrations up to
500 10 μM MC-LR induced significant enhancement of ROS levels at early times, reaching
501 the highest levels at 3 h after the exposure. Nonetheless, these authors also found that

after this time, ROS levels started to decline to basal levels due to a rapid response of cells (differentiated PC12 cells) against MC-LR. Moreover, in the present study, GSH levels decreased after 24 h of exposure at all the concentrations assayed. This could confirm the fact that ROS levels appeared unaffected since GSH could act directly against ROS (Circu and Aw, 2010). These oxidative stress parameters were not evaluated in differentiated SH-SY5Y cells since several authors have highlighted that these cells are more resistant to oxidative stressors due to changes in mitochondrial metabolism and antioxidant defenses (Cecchi et al., 2008; Cheung et al., 2009; Schneider et al., 2011). In contrast, diverse *in vivo* studies have reported the implication of oxidative stress in the neurotoxicity induced by MC-LR (Li et al., 2014 Mello et al., 2018, Wang et al., 2010; Zhao et al., 2015).

Concerning the AChE activity, this enzyme is a well-known biomarker of neuronal damage, as the affectation of the cholinergic system could lead to a malfunctioning of the locomotor system, behavior and cognitive processes (Kist et al., 2012). MCs may influence brain AChE indirectly via the inhibition of serine/threonine phosphatases (Hu et al., 2016). In our study, a significant increase of AChE activity was observed when undifferentiated SH-SY5Y cells were exposed to the highest concentration of MC-LR (37 μg/mL). The increased AChE activity could lead to a reduction of the cholinergic neurotransmission efficiency because of the lack of acetylcholine in the synaptic space, possibly contributing to a progressive cognitive impairment (Teodorak et al., 2015). Despite this, some other authors have demonstrated that AChE plays a role by promoting or suppressing cell death. An enhanced AChE activity take part in apoptosis, participating in the formation of apoptosomes or influencing the expression of apoptotic genes (Park et al., 2004; Ben-Ari et al., 2006; Zhu et al., 2007). Zhu et al. (2007) also stated that AChE expression during apoptosis is

527 associated with calcium mobilization. These facts are in agreement with our findings,
528 since it has been shown that MC-LR induced cell death by apoptosis at the highest
529 concentration assayed, correlating this effect with the AChE activity enhancement. On
530 the contrary, when differentiated SH-SY5Y cells were exposed to 45 µg/mL MC-LR,
531 no significant changes in the AChE activity were detected compared to the control
532 group. This could be due to structural and functional modifications of the cells after the
533 differentiation process, which could impede the effects of MC-LR over the AChE
534 activity. However, cell death by apoptosis was also observed in these cells, which
535 implies that not only the rise of the AChE could be involved in the cellular death, but
536 also other potential factors such as intracellular calcium levels etc., that should be
537 further investigated. Other authors have also evaluated the AChE activity disruption
538 induced by MC-LR, but their studies have been carried out in *in vivo* systems (Kist et
539 al., 2012; Qian et al., 2018; Wu et al., 2016; 2017), obtaining contradictory and not
540 conclusive results, depending on the administration route, or the experimental model
541 assayed, etc. Consequently, further research should be carried out in order to clarify the
542 effects of MCs on this key enzyme in the nervous system.

543 Concerning CYN, a very scarce number of studies have been carried out in order
544 to elucidate its neurotoxicity. However, due to its zwitterionic behavior and its small
545 size, CYN is likely to be taken by the cells through diffusion, being able the crossing
546 through the blood brain barrier (Florczyk et al., 2014; Valério et al. 2010). In the present
547 study, CYN showed EC_{50} values even lower than MC-LR both in undifferentiated and
548 differentiated cells. In agreement, Takser et al. (2016) found that pure CYN reached an
549 EC_{50} value between 0.1 and 10 µM CYN in N2a cells after 24, 48 and 72 h of exposure.
550 These authors also found that CYN induced almost a total cellular death at a
551 concentration of 10 µM in RAW264.7 and BV-2 cells. These findings are also in

552 agreement with the morphological results, which showed clear signs of cellular death by
553 apoptosis in both types of SH-SY5Y cells exposed to 1 µg/mL (2.4 µM) and 0.3 µg/mL
554 (0.7 µM) CYN. Relative to oxidative stress, although numerous works demonstrate *in*
555 *vitro* the oxidative stress induction by CYN in different cell lines (reviewed by Pichardo
556 et al., 2017), this work investigated the potential effects on ROS and GSH levels in the
557 undifferentiated SH-SY5Y cell line. However, no effects were found, which is in
558 disagreement with some *in vivo* studies, where oxidative stress was a main component
559 of the cellular damaged observed (Guzmán-Guillén et al., 2015; da Silva et al., 2018).
560 These discrepancies could be due to the different experimental model or the
561 concentrations used.

562 In relation to the AChE activity disruption, to our knowledge, no other papers
563 have been published concerning the effects of CYN on AChE activity *in vitro*. In the
564 present work, our results did not indicate any alteration at all CYN concentrations
565 assayed (up to 1 µg/mL) in undifferentiated cells. This is in agreement with da Silva et
566 al. (2018), who described no significant differences in the AChE activity in brain of fish
567 (*Hoplias malabaricus*) exposed to pure CYN after 7- and 14-days post treatment. In
568 addition, these authors also reported increased AChE activity by 44% in brain at 7 days
569 of exposure to aqueous CYN-producing cyanobacteria extracts, returning to control
570 levels after 14 days. However, when differentiated SH-SY5Y cells were exposed to 0-
571 0.3 µg/mL CYN, cultures showed a significant decrease of AChE activity at all CYN
572 concentrations. These observations are in agreement with the findings reported by
573 Guzmán-Guillén et al. (2015), who found a significant inhibition of 35% of AChE
574 activity in the brain of tilapia subchronically exposed to CYN (10 µg/L CYN) by
575 immersion in an *A. ovalisporum* culture for 14 days has been reported. In this study,
576 after a depuration process (7 days) a recovery of the enzyme was found. These contrary

577 responses could be due to differences in the experimental conditions, highlighting the
578 need to perform further studies.

579 Once the neurotoxic effects of pure MC-LR and CYN were studied separately, it
580 was interesting to study their effects in combination, since these toxins can appear
581 together in the nature (Bittencourt-Oliveira et al., 2014; Oehrle et al., 2010; Vasas et al.,
582 2004). In this sense, in the present work the MC-LR + CYN combination resulted more
583 cytotoxic than each individual toxin after 24 and 48 h of exposure in undifferentiated
584 SH-SY5Y cells. However, the differentiation process resulted in a lower cytotoxicity of
585 the toxin combination, as the effect of MC-LR + CYN was similar to that obtained for
586 MC-LR. The combination interaction was analyzed by the isobolograms method
587 described by Chou and Talalay (1984), which establish the foundations for assessing
588 whether cytotoxicity induced by a combination of cyanotoxins is more or less harmful
589 than the expected for individual cyanotoxins. This method is independent of the mode
590 of action of the compounds and considers both the potency (EC_{50}, *Dm*) and the shape
591 (*m*) of the dose-effect curve for each toxin (Ruiz et al., 2011a; 2011b). The method
592 allows a prediction of synergism/antagonism at all effect levels (*fa*) for a combination of
593 a different number of cyanotoxins. Depending on the equipotency level of MC-LR and
594 CYN, it is feasible the cyanotoxin interaction can vary between antagonism and
595 additivity. To explore this, the IC values at 50% inhibition (IC_{50}) and 90% inhibition
596 (IC_{90}) were determined. The combined effect of the combination observed on
597 undifferentiated SH-SY5Y cells is of antagonistic nature, with a slightly tendency to
598 additivity at higher concentrations. In differentiated cells, only an antagonistic behavior
599 was observed. However, experimental cytotoxicity and histopathological changes
600 obtained by the combination appeared to be more related with additivity than
601 antagonism in both cell types, although the antagonistic effect seems to be probable

602 since the effect of the combination was not as intense as it could be expected. Similar
603 results were obtained by Gutiérrez-Praena et al. (2018) in the hepatic cell line HepG2,
604 where the combination of both cyanotoxins also presented an antagonistic response in
605 the cells. This response could be due to complex dissimilar actions of these different
606 cyanotoxins, although the mechanisms of interaction remain unknown. However, it is
607 difficult to give an explanation to this phenomenon because of the isobolograms method
608 only allows quantitative determination of synergism or antagonism, and the elucidation
609 of the mechanism by which these relations occur is a separate issue that requires a
610 different kind of approach (Lu et al., 2013). Similar to our results, Takser et al. (2016)
611 found that a combination of MC-LR, CYN and anatoxin-a in an equimolar proportion
612 (3.33 μM) induced a significant reduction of cell viability in N2a cells after 24, 48 and
613 72 h of exposure. Moreover, these authors also found that this combination induced a
614 total cell death in the RAW264.7 and BV-2 cell lines. They also suggested that the
615 combination was more toxic compared with the individual compounds. Regarding cell
616 death, Takser et al. (2016) showed that the combination induced clear signs of cell
617 apoptosis in all the cell lines used. This is in agreement with our morphological results,
618 where an intense cell death was observed at the highest concentrations of the
619 combination assayed for both SH-SY5Y cell types (37 μg/mL MC-LR + 1 μg/mL CYN
620 and 45 μg/mL MC-LR + 0.3 μg/mL CYN for undifferentiated and differentiated
621 cultures, respectively), mainly by apoptosis. Concerning oxidative stress and the AChE
622 activity, no significant changes were observed respect to the control group at any of the
623 combination concentrations assayed in the undifferentiated cells. However, in the
624 differentiated SH-SY5Y cells a significant increase of AChE activity was observed at
625 the highest combination concentration (45 μg/mL MC-LR + 0.3 μg/mL CYN), which
626 could lead to the consequences previously described. To our knowledge, this is the first

627 report concerning these toxicological parameters, obtaining different responses after the
628 exposure to the combination and to the isolated toxins, highlighting the importance of
629 considering more realistic exposure-scenarios. Therefore, further investigations would
630 be needed to clarify the effects of the MC-LR-CYN-combination on neuronal cells, and
631 in different experimental models.

632

633 **5. Conclusions**

634 Our results showed a cytotoxic effect caused by the exposure to MC-LR and
635 CYN individually and in combination in both undifferentiated and differentiated SH-
636 SY5Y cells. CYN resulted more cytotoxic than MC-LR, but the combination presented
637 the highest cytotoxicity. However, the isobolograms method establishes that these
638 toxins together induce, mainly, an antagonistic response. Concerning oxidative stress
639 biomarkers, only MC-LR and the combination decreased GHS levels at the highest
640 concentration assayed. Moreover, AChE activity also showed different results for
641 individual toxins and their combination. The morphology study corroborated those
642 results observed with the cytotoxicity assays, since cell death by apoptosis was observed
643 at almost all the concentrations assayed of both toxins and the combination. Taking all
644 this into account, both cyanotoxins seem to present neurotoxic effects in the SH-SY5Y
645 cell line. Thus, as the potential neurotoxicity induced by MC-LR and CYN is of interest,
646 more studies concerning the different mechanisms by which both cyanotoxins can cross
647 the blood-brain barrier (diffusion, transporters, direct affectation of the barrier, etc.)
648 would be required. In addition, the affinity of these two cyanotoxins by the different
649 cells composing the nervous system would be also of interest, together with the study of

650 the toxic mechanisms these cyanotoxins can exert and their changes when single and
651 combination toxin exposure are considered.

652 **Acknowledgements**

653 The authors wish to thank the Ministerio de Economía y Competitividad of
654 Spain (AGL2015-64558-R, MINECO/FEDER, UE) for the financial support, the Junta
655 de Andalucia for the contact of María Gracia Hinojosa (USE-16667), and the Cell
656 Culture Service and Microscopy Service of Centro de Investigación, Tecnología e
657 Innovación from Universidad de Sevilla (CITIUS), for providing technical assistance.

658
659
660
661
662
663
664
665
666
667
668
669
670
671

672 **References**

673 Azevedo SMFO, Carmichael WW, Jochimsen EM, Rinehart KL, Lau S, Shaw GR,
674 Eaglesham GK. Human intoxication by microcystins during renal dialysis
675 treatment in Caruaru - Brazil. Toxicology. 2002; 181–182:441–6. Doi:
676 10.1016/S0300-483X(02)00491-2

677 Baganz D, Staaks G, Pflugmacher S, Steinberg CEW. Comparative study of
678 microcystin-LR-induced behavioral changes of two fish species, *Danio rerio* and
679 *Leucaspius delineatus*. Environ Toxicol. 2004; 19:564–70. Doi:
680 10.1002/tox.20063

681 Barltrop JA, Owen TC, Cory AH, Cory JG. 5-(3-carboxymethoxyphenyl)-2-(4,5-
682 dimethylthiazolyl)-3-(4-sulfophenyl)te trazolium, inner salt (MTS) and related
683 analogs of 3-(4,5-dimethylthiazolyl)-2,5-diphenyltetrazolium bromide (MTT)
684 reducing to purple water-soluble formazans as cell-viability indicators.
685 Bioorganic Med Chem Lett. 1991; 1:611–4. Doi: 10.1016/S0960-
686 894X(01)81162-8

687 Banker R, Carmeli S, Hadas O, Teltsch B, Porat R, Sukenik A. Identification of
688 cylindrospermopsin in *Aphanizomenon ovalisporum* (cyanophyceae) isolated
689 from Lake Kinneret, Israel. J Phycol. 1997; 33:613–6. Doi: 10.1111/j.0022-
690 3646.1997.00613.x

691 Ben-Ari S, Toiber D, Sas AS, Soreq H, Ben-Shaul Y. Modulated splicing-associated
692 gene expression in P19 cells expressing distinct acetylcholinesterase splice
693 variants. J Neurochem. 2006; 97 Suppl 1:24–34. Doi: 10.1111/j.1471-
694 4159.2006.03725.x

695 Bittencourt-Oliveira MDC, Piccin-Santos V, Moura AN, Aragão-Tavares NKC,
696 Cordeiro-Araújo MK. Cyanobacteria, microcystins and cylindrospermopsin in
697 public drinking supply reservoirs of Brazil. An Acad Bras Cienc. 2014; 86:297–
698 309. Doi: 10.1590/0001-3765201302512

699 Bogialli S, Bruno M, Curini R, Di Corcia A, Fanali C, Laganà A. Monitoring algal
700 toxins in lake water by liquid chromatography tandem mass spectrometry.
701 Environ Sci Technol. 2006; 40:2917–23. Doi: 10.1021/es052546x

702 Borenfreund E, Puerner JA. Toxicity determined *in vitro* by morphological alterations
703 and neutral red absorption. Toxicol Lett. 1985; 24:119–24. Doi: 10.1016/0378-
704 4274(85)90046-3

705 Bourke ATC, Hawes RB, Neilson A, Stallman ND. An outbreak of hepato-enteritis (the
706 Palm Island mystery disease) possibly caused by algal intoxication. Toxicon.
707 1983; 21:45–8. Doi: 10.1016/0041-0101(83)90151-4

708 Bradford MM. A rapid and sensitive method for the quantitation of microgram
709 quantities of protein utilizing the principle of protein-dye binding. Anal
710 Biochem. 1976; 72:248–54. Doi: 10.1016/0003-2697(76)90527-3

711 Buratti FM, Manganelli M, Vichi S, Stefanelli M, Scardala S, Testai E, Funari E.
712 Cyanotoxins: producing organisms, occurrence, toxicity, mechanism of action
713 and human health toxicological risk evaluation. Arch Toxicol. 2017; 91:1049–
714 130. Doi: 10.1007/s00204-016-1913-6

715 Cai F, Liu J, li C, Wang J. Intracellular calcium plays a critical role in the microcystin-
716 lr-elicited neurotoxicity through PLC/IP3 pathway. Int J Toxicol. 2015; 34:551–
717 8. Doi: 10.1177/1091581815606352

718 Carmichael WW, Azevedo SMFO, An JS, Molica RJR, Jochimsen EM, Lau S, Rinehart
719 KL, Shaw GR, Eaglesham GK. Human fatalities form cyanobacteria: Chemical
720 and biological evidence for cyanotoxins. Environ Health Perspect. 2001;
721 109:663–8. Doi: 10.1289/ehp.01109663

722 Cecchi C, Pensalfini A, Liguri G, Baglioni S, Fiorillo C, Guadagna S, Zampagni M,
723 Formigli L, Nosi D, Stefani M. Differentiation increases the resistance of
724 neuronal cells to amyloid toxicity. Neurochem Res. 2008; 33:2516–31. Doi:
725 10.1007/s11064-008-9627-7

726 Chen L, Xie P. Mechanisms of Microcystin-induced cytotoxicity and apoptosis. Mini-
727 Reviews Med Chem. 2016;16:1018–31. Doi: 10.1016/j.aquatox.2014.01.021

728 Cheung YT, Lau WKW, Yu MS, Lai CSW, Yeung SC, So KF, Chang RCC. Effects of
729 all-trans-retinoic acid on human SH-SY5Y neuroblastoma as *in vitro* model in
730 neurotoxicity research. Neurotoxicol. 2009; 30:127-135. Doi:
731 10.1016/j.neuro.2008.11.001

732 Chou T. Theoretical basis, experimental design, and computerized simulation of
733 synergism and antagonism in drug combination studies. Pharmacol Rev. 2006;
734 58:621–81. Doi: 10.1124/pr.58.3.10.

735 Chou TC, Talalay P. Quantitative analysis of dose-effect relationships: the combined
736 effects of multiple drugs or enzyme inhibitors. Adv Enzyme Regul. 1984;
737 22:27–55. Doi: 10.1016/0065-2571(84)90007-4

738 Circu ML, Aw TY. Reactive oxygen species, cellular redox systems, and apoptosis.
739 Free Radic Biol Med. 2010; 48:749–62. Doi:
740 10.1016/j.freeradbiomed.2009.12.022

741 Da Silva R de C, Grötzner SR, Moura Costa DD, Esquivel JR, Muelbert J, Freitas de
742 Magalhães V, Filipak F, de Oliveira CA. Comparative bioaccumulation and
743 effects of purified and cellular extract of cylindrospermopsin to freshwater fish
744 *Hoplias malabaricus*. J Toxicol Environ Heal - Part A Curr Issues. 2018;
745 81:620–32. Doi: 10.1080/15287394.2018.1469101

746 Ding J, Wang J, Xiang Z, Diao W, Su M, Shi W, Wan T, Han X. The organic anion
747 transporting polypeptide 1a5 is a pivotal transporter for the uptake of
748 microcystin-LR by gonadotropin-releasing hormone neurons. Aquat Toxicol.
749 2017; 182:1-10. Doi: 10.1016/j.aquatox.2016.11.005

750 Ellman, G. L., Courtney, K. D., Andres, V., & Featherstone, R. M. A new and rapid
751 colorimetric determination of acetylcholinesterase activity. *Biochem.*
752 *Pharmacol*. 1961; *7*:88–95. Doi: 10.1016/0006-2952(61)90145-9

753 Encinas M, Iglesias M, Liu Y, Wang H, Muhaisen A, Ceña V, Gallego C, Comella JX.
754 Sequential treatment of SH-SY5Y cells with retinoic acid and brain-derived
755 neurotrophic factor gives rise to fully differentiated, neurotrophic factor-
756 dependent human neuron-like cells. J Neurochem. 2000; 75:991-1003. Doi:
757 10.1046/j.1471-4159.2000.0750991.x

758 Falconer IR. An overview of problems caused by toxic blue – green algae
759 (cyanobacteria) in drinking and recreational water. Environ Toxicol. 1999; 14:5–
760 12. Doi: 10.1002/(SICI)1522-7278(199902)14:1<5::AID-TOX3>3.0.CO;2-0

761 Falconer IR, Humpage R. Cyanobacterial (blue-green algal) toxins in water supplies:
762 cylindrospermopsin. Environ Toxicol. 2006; 21:299-304. Doi:
763 10.1002/tox.20194

764 Feurstein D, Holst K, Fischer A, Dietrich DR. Oatp-associated uptake and toxicity of
765 microcystins in primary murine whole brain cells. Toxicol Appl Pharmacol.
766 2009; 234:247–55. Doi: 10.1016/j.taap.2008.10.011

767 Feurstein D, Stemmer K, Kleinteich J, Speicher T, Dietrich DR. Microcystin congener-
768 and concentration-dependent induction of murine neuron apoptosis and neurite
769 degeneration. Toxicol Sci. 2011; 124:424–31. Doi: 10.1093/toxsci/kfr243

770 Fischer WJ, Altheimer S, Cattori V, Meier PJ, Dietrich DR, Hagenbuch B. Organic
771 anion transporting polypeptides expressed in liver and brain mediate uptake of
772 microcystin. Toxicol Appl Pharmacol. 2005; 203:257–63. Doi:
773 10.1016/j.taap.2004.08.012

774 Florczyk M, Łakomiak A, Woźny M, Brzuzan P. Neurotoxicity of cyanobacterial
775 toxins. Environ Biotechnol. 2014; 10:26–43. Doi: 10.14799/ebms246

776 Froscio SM, Humpage AR, Burcham PC, Falconer IR. Cylindrospermopsin-induced
777 protein synthesis inhibition and its dissociation from acute toxicity in mouse
778 hepatocytes. Environ Toxicol. 2003; 18:243–51. Doi: 10.1002/tox.10121

779 Gutiérrez-Praena D, Pichardo S, Jos Á, María Cameán A. Toxicity and glutathione
780 implication in the effects observed by exposure of the liver fish cell line PLHC-1
781 to pure cylindrospermopsin. Ecotoxicol Environ Saf. 2011; 74:1567–72. Doi:
782 10.1016/j.ecoenv.2011.04.030

783 Gutiérrez-Praena D, Pichardo S, Jos Á, Moreno FJ, Cameán AM. Biochemical and
784 pathological toxic effects induced by the cyanotoxin Cylindrospermopsin on the
785 human cell line Caco-2. Water Res. 2012; 46:1566–75. Doi:
786 10.1016/j.watres.2011.12.044

787 Gutiérrez-Praena D, Guzmán-Guillén R, Pichardo S, Moreno FJ, Vasconcelos V, Jos A,
788 Cameán AM. Cytotoxic and morphological effects of microcystin-LR,
789 cylindrospermopsin, and their combinations on the human hepatic cell line
790 HepG2. Environ Toxicol. 2018; 34:1-12. Doi: 10.1002/tox.22679

791 Guzmán-Guillén R, Prieto AI, Vasconcelos VM, Cameán Fernandez AM.
792 Cyanobacterium producing cylindrospermopsin cause histopathological changes
793 at environmentally relevant concentrations in subchronically exposed tilapia
794 (*Oreochromis niloticus*). Environ Toxicol. 2013; 90:1184–94. Doi:
795 10.1002/tox.21904

796 Guzmán-Guillén R, Manzano IL, Moreno IM, Ortega AIP, Moyano R, Blanco A,
797 Cameán AM. Cylindrospermopsin induces neurotoxicity in tilapia fish
798 (*Oreochromis niloticus*) exposed to *Aphanizomenon ovalisporum*. Aquat
799 Toxicol. 2015; 161:17–24. Doi: 10.1016/j.aquatox.2015.01.024

800 Harada K ichi, Ohtani I, Iwamoto K, Suzuki M, Watanabe MF, Watanabe M, Terao K.
801 Isolation of cylindrospermopsin from a cyanobacterium *Umezakia natans* and its
802 screening method. Toxicon. 1994; 32:73–84. Doi: 10.1016/0041-
803 0101(94)90023-X

804 Hawkins PR, Runnegar MTC, Jackson ARB, Falconer IR. Severe hepatotoxicity caused
805 by the tropical cyanobacterium supply reservoir. Appl Environ Microbiol. 1985;
806 50:1292–5. Doi: 10.1016/S1383-5718(00)00144-3

807 Hu Y, Chen J, Fan H, Xie P, He J. A review of neurotoxicity of microcystins. Environ
808 Sci Pollut Res. 2016; 23:7211–9. Doi: 10.1007/s11356-016-6073-y

809 Humpage AR, Fontaine F, Froscio S, Burcham P, Falconer IR. Cylindrospermopsin
810 genotoxicity and cytotoxicity: Role of cytochrome P-450 and oxidative stress. J
811 Toxicol Environ Heal - Part A. 2005; 68:739–53.

812 Jos A, Cameán AM, Pflugmacher S, Segner H. The antioxidant glutathione in the fish
813 cell lines EPC and BCF-2: response to model pro-oxidants as measured by three
814 different fluorescent dyes. Toxicol In Vitro. 2009; 23:546-53.

815 Kinnear SH, Fabbro LD, Duivenvoorden LJ, Hibberd EM. Multiple-organ toxicity
816 resulting from cylindrospermopsin exposure in tadpoles of the cane toad (*Bufo*
817 *marinus*). Environ Toxicol. 2007; 22:550-8. Doi: 10.1002/tox.20299

818 Kiss T, Vehovszky Á, Hiripi L, Kovács A, Vörös L. Membrane effects of toxins
819 isolated from a cyanobacterium, *Cylindrospermopsis raciborskii*, on identified
820 molluscan neurones. Comp Biochem Physiol - C Toxicol Pharmacol. 2002;
821 131:167–76. Doi: 10.1016/S1532-0456(01)00290-3

822 Kist LW, Rosemberg DB, Pereira TCB, De Azevedo MB, Richetti SK, De Castro Leão
823 J, Sarkis Yunes J, Bonan CD, Bogo MR. Microcystin-LR acute exposure
824 increases AChE activity via transcriptional ache activation in zebrafish (*Danio*
825 *rerio*) brain. Comp Biochem Physiol - C Toxicol Pharmacol; 2012; 155:247–52.
826 Doi: 10.1016/j.cbpc.2011.09.002

827 Li G, Cai F, Yan W, Li C, Wang J. A proteomic analysis of MCLR-induced
828 neurotoxicity: Implications for Alzheimer's disease. Toxicol Sci. 2012;
829 127:485–95. Doi: 10.1093/toxsci/kfs114

830 Li XB, Zhang X, Ju J, Li Y, Yin L, Pu Y. Alterations in neurobehaviors and
831 inflammation in hippocampus of rats induced by oral administration of

832 microcystin-LR. Environ Sci Pollut Res. 2014; 21:12419–25. Doi:
833 10.1007/s11356-014-3151-x

834 Li X, Zhang X, Ju J, Li Y, Yin L, Pu Y. Maternal repeated oral exposure to microcystin-
835 LR affects neurobehaviors in developing rats. Environ Toxicol Chem. 2015;
836 34:64–9. doi:10.1002/etc.2765

837 Liu W, Chen C, Chen L, Wang L, Li J, Chen Y, Jin J, Kawan A, Zhang X. Sex-
838 dependent effects of microcystin-LR on hypothalamic-pituitary-gonad axis and
839 gametogenesis of adult zebrafish. Sci Rep. 2016; 6:1–12. Doi :
840 10.1038/srep22819

841 Lu H, Fernández-Franzón M, Font G, Ruiz MJ. Toxicity evaluation of individual and
842 mixed enniatins using an *in vitro* method with CHO-K1 cells. Toxicol In Vitro.
843 2013; 27:672–80. Doi: 10.1016/j.tiv.2012.11.009

844 MacKintosh C, Beattie KA, Klumpp S, Cohen P, Codd GA. Cyanobacterial
845 microcystin-LR is a potent and specific inhibitor of protein phosphatases 1 and
846 2A from both mammals and higher plants. Febs. 1990; 264:187–92. Doi:
847 10.1016/0014-5793(90)80245-E

848 Malbrouck C, Kestemont P. Effects of microcystins on fish. Environ Toxicol Chem.
849 2006; 25:72–86. Doi: 10.1897/05-029R.1

850 McLellan NL, Manderville RA. Toxic mechanisms of microcystins in mammals.
851 Toxicol Res (Camb). 2017; 6:391–405. Doi: 10.1039/c7tx00043j

852 Menezes C, Alverca E, Dias E, Sam-Bento F, Pereira P. Involvement of endoplasmic
853 reticulum and autophagy in microcystin-LR toxicity in Vero-E6 and HepG2 cell
854 lines. Toxicol In Vitro. 2013; 27:138–48. Doi: 10.1016/j.tiv.2012.09.009

855 Meng G, Sun Y, Fu W, Guo Z, Xu L. Microcystin-LR induces cytoskeleton system
856 reorganization through hyperphosphorylation of tau and HSP27 via PP2A
857 inhibition and subsequent activation of the p38 MAPK signaling pathway in
858 neuroendocrine (PC12) cells. Toxicology. 2011; 290:219–29. Doi:
859 10.1016/j.tox.2011.09.085

860 Meng G, Liu J, Lin S, Guo Z, Xu L. Microcystin-LR-caused ROS generation involved
861 in p38 activation and tau hyperphosphorylation in neuroendocrine (PC12) cells.
862 Environ Toxicol. 2013; 30:366-74. Doi: 10.1002/tox.21914

863 Mello FD, Braidy N, Marçal H, Guillemin G, Nabavi SM, Neilan BA. Mechanisms and
864 Effects Posed by Neurotoxic Products of Cyanobacteria/Microbial
865 Eukaryotes/Dinoflagellates in Algae Blooms: a Review. Neurotox Res. 2018;
866 33(1):153–67. Doi: 10.1007/s12640-017-9780-3

867 Oehrle SA, Southwell B, Westrick J. Detection of various freshwater cyanobacterial
868 toxins using ultra-performance liquid chromatography tandem mass
869 spectrometry. Toxicon. 2010; 55:965–72. Doi:10.1016/j.toxicon.2009.10.001

870 Park SE, Kim ND, Yoo YH. Acetylcholinesterase plays a pivotal role in apoptosome
871 formation. Cancer Res. 2004; 64:2652–5. Doi:10.1158/0008-5472.CAN-04-
872 0649

873 Pichardo S, Jos A, Zurita JL, Salguero M, Camean AM, Repetto G. The use of the fish
874 cell lines RTG-2 and PLHC-1 to compare the toxic effects produced by
875 microcystins LR and RR. Toxicol In Vitro. 2005; 19:865–73. Doi:
876 10.1016/j.tiv.2005.06.016

877 Pichardo S, Cameán AM, Jos A. *In vitro* toxicological assessment of
878 cylindrospermopsin: A review. Toxins (Basel). 2017; 9(12). Doi:
879 10.3390/toxins9120402

880 Pouria S, De Andrade A, Barbosa J, Cavalcanti RL, Barreto VTS, Ward CJ. Fatal
881 microcystin intoxication in haemodialysis unit in Caruaru, Brazil. Lancet. 1998;
882 352:21–6. Doi: 10.1016/S0140-6736(97)12285-1

883 Puerto M, Pichardo S, Jos Á, Prieto AI, Sevilla E, Frías JE, Cameán AM. Differential
884 oxidative stress responses to pure Microcystin-LR and Microcystin-containing
885 and non-containing cyanobacterial crude extracts on Caco-2 cells. Toxicon.
886 2010; 55:514–22. Doi: 10.1016/j.toxicon.2009.10.003

887 Puerto M, Gutiérrez-Praena D, Prieto AI, Pichardo S, Jos A, Miguel-Carrasco JL,
888 Vázquez CM, Cameán AM. Subchronic effects of cyanobacterial cells on the
889 transcription of antioxidant enzyme genes in tilapia (*Oreochromis niloticus*).
890 Ecotoxicology. 2011; 20:479–90. Doi: 10.1007/s10646-011-0600-x

891 Puerto M, Prieto AI, Maisanaba S, Gutiérrez-Praena D, Mellado-García P, Jos Á, et al.
892 Mutagenic and genotoxic potential of pure Cylindrospermopsin by a battery of
893 *in vitro* tests. Food Chem Toxicol. 2018; 121:413–22. Doi:
894 10.1016/j.fct.2018.09.013

895 Qian H, Liu G, Lu T, Sun L. Developmental neurotoxicity of *Microcystis aeruginosa* in
896 the early life stages of zebrafish. Ecotoxicol Environ Saf. 2018; 151:35–41. Doi:
897 10.1016/j.ecoenv.2017.12.059

898 Qiu T, Xie P, Liu Y, Li G, Xiong Q, Hao L, et al. The profound effects of microcystin
899 on cardiac antioxidant enzymes, mitochondrial function and cardiac toxicity in
900 rat. Toxicology. 2009; 257:86–94. Doi: 10.1016/j.tox.2008.12.012

Ruiz MJ, Macáková P, Juan-García A, Font G. Cytotoxic effects of mycotoxin combinations in mammalian kidney cells. Food Chem Toxicol. 2011a; 49(10):2718–24. Doi: 10.1016/j.fct.2011.07.021

Ruiz MJ, Franzova P, Juan-García A, Font G. Toxicological interactions between the mycotoxins beauvericin, deoxynivalenol and T-2 toxin in CHO-K1 cells in vitro. Toxicon. 2011b; 58:315–26. Doi: 10.1016/j.toxicon.2011.07.015

Rozman KB, Jurič DM, Šuput D. Selective cytotoxicity of microcystins LR, LW and LF in rat astrocytes. Toxicol Lett. 2017; 265:1–8. Doi: 10.1016/j.toxlet.2016.11.008

Santillo MF, Liu Y. A fluorescence assay for measuring acetylcholinesterase activity in rat blood and a human neuroblastoma cell line (SH-SY5Y). J Pharmacol Toxicol Methods. 2015; *76*:15–22. Doi: 10.1016/j.vascn.2015.07.002

Schembri M a, Neilan B a, Saint CP. Identification of genes implicated in toxin production in the cyanobacterium *Cylindrospermopsis raciborskii.* Environ Toxicol. 2001; 16:413–21. Doi: 10.1002/tox.1051

Schneider L, Giordano S, Zelickson BR, Johnson MS, Benavides GA, Ouyang X, Fineberg N, Darley-Usmar VM, Zhang J. Differentiation of SH-SY5Y cells to a neuronal phenotype changes cellular bioenergetics and the response to oxidative stress. Free Rad Biol Med. 2011; 51:2007-17. Doi: 10.1016/j.freeradbiomed.2011.08.030

Shaw GR, Sukenik A, Livne A, Chiswell RK, Smith MJ, Seawright AA, Norris RL, Eaglesham GK, Moore MR. Blooms of the cylindrospermopsin containing cyanobacterium, *Aphanizomenon ovalisporum* (Fofti), in newly constructed lakes, Queensland, Australia. Environ Toxicol. 1999; 14:167–77. Doi: 10.1002/(SICI)1522-7278(199902)14:1<167::AID-TOX22>3.0.CO;2-O

925 Sivonen K and Jones G. Cyanobacterial toxins. In: Chorus, I. and Bartram, J., Eds.,
926 Toxic cyanobacteria in water: a guide to their public health consequences,
927 monitoring, and management, E & FN Spon. 1999, 41-111.

928 Spoof L, Catherine A. Appendix 3, in: Meriluto J, Spoof L, Codd GA. Handbook of
929 cyanobacterial monitoring and cyanotoxin analysis. 2017; 526-537.

930 Svirčev ZB, Tokodi N, Drobac D, Codd GA. Cyanobacteria in aquatic ecosystems in
931 Serbia: Effects on water quality, human health and biodiversity. Syst Biodivers.
932 2014; 12:261–70. Doi: 10.1080/14772000.2014.921254

933 Tait SWG, Green DR. Mitochondrial regulation of cell death. Cold Spring Harb
934 Perspect Biol. 2013; 5:1-15. Doi: 10.1101/cshperspect.a008706

935 Takser L, Benachour N, Husk B, Cabana H, Gris D. Cyanotoxins at low doses induce
936 apoptosis and inflammatory effects in murine brain cells: Potential implications
937 for neurodegenerative diseases. Toxicol Reports. 2016; 3:180–9. Doi:
938 10.1016/j.toxrep.2015.12.008

939 Tatay E, Meca G, Font G, Ruiz MJ. Interactive effects of zearalenone and its
940 metabolites on cytotoxicity and metabolization in ovarian CHO-K1 cells.
941 Toxicol In Vitro. 2014; 28:95–103. Doi: 10.1016/j.tiv.2013.06.025

942 Terao K, Ohmori S, Igarashi K, Ohtani I, Watanabe MF, Harada KI, Ito E, Watanabe
943 M. Electron microscopic studies on experimental poisoning in mice induced by
944 cylindrospermopsin isolated from blue-green algae *Umezakia natans*. Toxicon.
945 1994; 32:833–43. Doi: 10.1016/0041-0101(94)90008-6

946 Testai E, Buratti FM, Funari E, Manganelli M, Vichi S, Arnich N, et al. Review and
947 analysis of occurrence, exposure and toxicity of cyanobacteria toxins in food.
948 EFSA Support Publ. 2016; 13:1-309. Doi: 10.2903/sp.efsa.2016.EN-998

949 Valério E, Chaves S, Tenreiro R. Diversity and impact of prokaryotic toxins on aquatic
950 environments: A review. Toxins. 2010; 2:2359–410. Doi:
951 10.3390/toxins2102359

952 Vasas G, Gáspár A, Páger C, Surányi G, Máthé C, Hamvas MM, Borbely G. Analysis
953 of cyanobacterial toxins (anatoxin-a, cylindrospermopsin, microcystin-LR) by
954 capillary electrophoresis. Electrophoresis. 2004; 25:108–15. Doi:
955 10.1002/elps.200305641

956 Wang M, Wang D, Lin L, Hong H. Protein profiles in zebrafish (*Danio rerio*) brains
957 exposed to chronic microcystin-LR. Chemosphere. 2010; 81:716–24. Doi:
958 10.1016/j.chemosphere.2010.07.061

959 Wang J, Lin F, Cai F, Yan W, Zhou Q, Xie L. Microcystin-LR inhibited hippocampal
960 long-term potential via regulation of the glycogen synthase kinase-3β pathway.
961 Chemosphere. 2013; 93:223–9. Doi: 10.1016/j.chemosphere.2013.04.069

962 White SH, Duivenvoorden LJ, Fabbro LD, Eaglesham GK. Mortality and toxin
963 bioaccumulation in *Bufo marinus* following exposure to *Cylindrospermopsis*
964 *raciborskii* cell extracts and live cultures. Environ Pollut. 2007; 147:158–67.
965 Doi: 10.1016/j.envpol.2006.08.010

966 Wu Q, Yan W, Liu C, Li L, Yu L, Zhao S, Li G. Microcystin-LR exposure induces
967 developmental neurotoxicity in zebrafish embryo. Environ Pollut. 2016;
968 213:793–800. Doi: 10.1016/j.envpol.2016.03.048

969 Wu Q, Yan W, Cheng H, Liu C, Hung TC, Guo X, Li G. Parental transfer of
970 microcystin-LR induced transgenerational effects of developmental
971 neurotoxicity in zebrafish offspring. Environ Pollut. 2017; 231:471–8. Doi:
972 10.1016/j.envpol.2017.08.038

973 Xie HR, Hu LS, Li GY. SH-SY5Y human neuroblastoma cell line: in vitro cell model
974 of dopaminergic neurons in Parkinson's disease. Chin Med J. 2010; 123:1086-
975 92. Doi: 10.3760/cma.j.issn.0366-6999.2010.08.021

976 Yagdiran Y, Oskarsson A, Knight CH, Tallkvist J. ABC- and SLC-transporters in
977 murine and bovine mammary epithelium – Effects of Prochloraz. .PLoSONE.
978 2016; 11:e0151904. Doi: 10.1371/journal.pone.0151904

979 Žegura B, Štraser A, Filipič M. Genotoxicity and potential carcinogenicity of
980 cyanobacterial toxins - a review. Mutat Res - Rev Mutat Res. 2011; 727:16–41.
981 Doi: 10.1016/j.mrrev.2011.01.002

982 Zeng C, Sun H, Xie P, Wang J, Zhang G, Chen N, et al. The role of apoptosis in
983 MCLR-induced developmental toxicity in zebrafish embryos. Aquat Toxicol.
984 2014; 149:25–32. Doi: 10.1016/j.aquatox.2014.01.021

985 Zhang Y, Zhang J, Wang E, Qian W, Fan Y, Feng Y, Yin H, Li Y, Wang Y, Yuan T.
986 microcystin-leucine-arginine induces tau pathology through bα degradation via
987 protein phosphatase 2a demethylation and associated glycogen synthase kinase-
988 3β phosphorylation. Toxicol Sci. 2018; 162:475–87. Doi: 10.1093/toxsci/kfx271

989 Zhao S, Li G, Chen J. A proteomic analysis of prenatal transfer of microcystin-LR
990 induced neurotoxicity in rat offspring. J Proteomics. 2015; 114:197–213. Doi:
991 10.1016/j.jprot.2014.11.015

992 Zhu H, Gao W, Jiang H, Jin QH, Shi YF, Tsim KW, Zhang XJ. Regulation of
993 acetylcholinesterase expression by calcium signaling during calcium ionophore
994 A23187- and thapsigargin-induced apoptosis. Int J Biochem Cell Biol. 2007;
995 39:93–108. Doi: 10.1016/j.biocel.2006.06.012

Figure captions

Figure 1. Reduction of tetrazolium salt (MTS), neutral red uptake (NR) and protein content (PC) on SH-SY5Y cells after 24 h (**A**) and 48 h (**B**) of exposure to 0-100 µg/mL MC-LR. All values are expressed as mean ± s.d. ** MTS significantly different from control group ($p<0.01$), §§ all parameters significantly different from control group ($p<0.01$).

Figure 2. Reduction of tetrazolium salt (MTS), neutral red uptake (NR) and protein content (PC) on SH-SY5Y cells after 24 h (**A**) and 48 h (**B**) of exposure to 0-10 µg/mL CYN. All values are expressed as mean ± s.d. ** MTS significantly different from control group ($p<0.01$), ¥ NR significantly different from control group ($p<0.05$), §§ all parameters significantly different from control group ($p<0.01$).

Figure 3. Reduction of tetrazolium salt (MTS) on SH-SY5Y cells after 24 h (**A**) and 48 h (**B**) of exposure to different concentrations of MC-LR + CYN combinations at a ratio of CE_{50} MC-LR / CE_{50} CYN (37:1). All values are expressed as mean ± s.d. ** significantly different from control ($p<0.01$) for the three toxins tested, and ¥¥ significantly different from control group ($p<0.01$) for the MC-LR toxin alone.

Figure 4. Combination index (CI)/fraction affected (fa) curve in undifferentiated (**A, B**) and differentiated (**C, D**) SH-SY5Y cells exposed to a MC-LR and CYN binary combination after 24 h and 48 h of exposure. Each point represents the CI ± s.d. at a fractional effect. The dotted line (CI = 1) indicates additivity, the area under the dotted line points out a synergist effect, and the area above the dotted line signify antagonism.

Figure 5. Reactive oxygen species (ROS) and reduced glutathione (GSH) levels on SH-SY5Y cells after 4, 8, 12 and 24 hours of exposure to 0-37 µg/mL MC-LR. Cells exposed to medium without serum were used as negative control in both assays (C-). Cells exposed to 200 µM $MnCl_2 \cdot 4H_2O$ and exposed to 1 µM BSO were used as positive control (C+) in the case of the ROS and the GSH assays, respectively. All values are expressed as mean ± s.d. The significance levels observed are * $p<0.05$ and ** $p<0.01$ significantly different from control group.

Figure 6. Reactive oxygen species (ROS) and reduced glutathione (GSH) levels on SH-SY5Y clls after 4, 8, 12 and 24 hours of exposure to 0-1 µg/mL CYN. Cells exposed to medium without serum were used as negative control in both assays (C-). Cells exposed to 200 µM $MnCl_2 \cdot 4H_2O$ and exposed to 1 µM BSO were used as positive

control (C+) in the case of the ROS and the GSH assays, respectively. All values are expressed as mean ± s.d. ** Significantly different from control group ($p<0.01$).

Figure 7. Reactive oxygen species (ROS) and reduced glutathione (GSH) levels on SH-SY5Y cells after 4, 8, 12 and 24 hours of exposure to different concentrations of MC-LR + CYN combinations at a ratio of CE_{50} MC-LR / CE_{50} CYN (37:1). Cells exposed to medium without serum were used as negative control in both assays (C-). Cells exposed to 200 µM $MnCl_2 \cdot 4H_2O$ and exposed to 1 µM BSO were used as positive control (C+) in the case of the ROS and the GSH assays, respectively. All values are expressed as mean ± s.d. The significance levels observed are * $p<0.05$ and ** $p<0.01$ significantly different from control group.

Figure 8. Acetylcholinesterase activity (AChE) on undifferentiated and differentiated SH-SY5Y cells exposed to MC-LR (0-37 or 0-45 µg/mL, respectively), CYN (0-1 or 0.3 µg/mL, respectively) or MC-LR + CYN combination after 24 h. Cells exposed to medium without serum were used as negative control in both assays (C-). Cells exposed to 50 nM parathion were used as positive control (C+). All values are expressed as mean ± s.d. ** Indicates significant difference from control group value ($p<0.01$).

Figure 9. Morphology of control undifferentiated SH-SY5Y cells after 24 h of exposure to nutrient medium without serum. Contrast-phase microscopy of a SH-SY5Y cell culture in normal neuronal growth. Cells present cytoplasmic projections contacting with other cells (arrows) and the morphological characteristics of an epithelial culture (arrowheads). Bar=50µm (**A**). Semithin sections of cells culture were stained with toluidine blue. Cells in mitosis processes (arrows) with big nucleoli in the nucleus (arrowheads). Bar=25µm (**B**). Transmission electronic microscopy of SH-SY5Y cells with euchromatic nuclei (N) and dense nucleoli (n). Free ribosomes (asterisk) and scarce mitochondria (arrows). Bar=2 µm (**C**).

Figure 10. Morphology of control differentiated SH-SY5Y cells after 24 h of exposure to nutrient medium without serum. Contrast-phase microscopy of a SH-SY5Y cell culture in normal neuronal growth. Cells present cytoplasmic projections contacting with other cells (arrows). Bar=100µm (**A**). Semithin sections of cells culture were stained with toluidine blue. Cells in mitosis processes (asterisk). Endoplasmic reticulum dilatations (arrowheads) and lipidic vacuoles (arrows). Bar=25µm (**B**). Transmission

electronic microscopy of SH-SY5Y cells presenting numerous microtubules and intermediate filaments (arrowheads). Bar=2 µm (**C**).

Figure 11. Morphology of undifferentiated SH-SY5Y cells after 24 h of exposure to MC-LR. Phase-contrast microscopy of cells exposed to 37 µg/mL MC-LR. Rounded cells (arrows) with clear signs of cell death. Bar=50 µm (**A**). Semithin sections of cells culture were stained with toluidine blue. Cells exposed to 37 µg/mL MC-LR. Nuclei with condensed chromatin (arrows) as clear sign of cell death. Bar=20 µm (**B**). Transmission electronic microscopy of SH-SY5Y cells exposed to 37 µg/mL MC-LR. Irregular nuclei (N), pseudopods retraction, appearance of blisters in the cellular membrane (arrows), and presence of apoptotic bodies (arrowheads). Chromatin condensation (Ch) and nucleolar segregation of apoptotic nuclei (N). Nucleolus (n).Bar=2.5 µm (**C, D**). Phase-contrast microscopy of cells exposed to 9.25 µg/mL MC-LR. Enlarged cells with cytoplasmic elongations as lamellipodiums (arrows). Bar=50 µm (**E**). Semithin sections of cells culture were stained with toluidine blue. Cells exposed to 18.5 µg/mL MC-LR. Cells with irregular shape (arrows) presenting big nucleoli (arrowheads). Bar=20 µm (**F**). Transmission electronic microscopy of SH-SY5Y cells exposed to 18.5 and 9.25 µg/mL MC-LR. Altered mitochondria rounded by endoplasmic reticulum cisternae (arrows) forming autophagosomes (asterisk). Euchromatic nucleus (N) with a big nucleolus (n) where it is possible to observe the granulas component (GC), the dense fibrillary component (DFC) and the fibrillary center (FC). Bar=2 µm (**G, H**).

Figure 12. Morphology of differentiated SH-SY5Y cells after 24 h of exposure to MC-LR. Phase-contrast microscopy of cells exposed to 45 µg/mL MC-LR. Rounded cells (arrows) with clear signs of cell death. Bar=100 µm (**A**). Semithin sections of cells culture were stained with toluidine blue. Cells exposed to 45 µg/mL MC-LR. Presence of numerous apoptotic bodies (arrows) as clear sign of cell death. Presence of dilated endoplasmic reticulum (arrowheads). Bar=25 µm (**B**). Transmission electronic microscopy of differentiated SH-SY5Y cells exposed to 45 µg/mL MC-LR. Chromatin condensation (Chr), presence of numerous mitochondria (Mit), and nucleolar segregation of apoptotic nuclei (N). Nucleolus (n).Bar=2.5 µm (**C, D**). Semithin sections of cells culture were stained with toluidine blue. Cells exposed to 22.5 µg/mL MC-LR. Enlarged cells with cytoplasmic elongations as lamellipodiums (arrows) and presence of apoptotic cellular debris (arrowheads). Bar=25 µm (**E, F**). Transmission

electronic microscopy of differentiated SH-SY5Y cells exposed to 22.5 µg/mL MC-LR. Cells with irregular shape presenting nuclei (N) with chromatin condensation (Chr). Bar=2 µm (**G**). Semithin sections of cells culture were stained with toluidine blue. Cells exposed to 11.25 µg/mL MC-LR. Numerous dilated endoplasmic reticuli (arrows) with protein condensation (arowheads). Bar=25 µm (**H**). Transmission electronic microscopy of differentiated SH-SY5Y cells exposed to 11.25 µg/mL MC-LR. Presence of mitochondria (Mit), protein condensation (arrowheads) and lipidic vacuoles (Lp). Bar=2 µm (**I, J**).

Figure 13. Morphology of undifferentiated SH-SY5Y cells after 24 h of exposure to CYN. Semithin sections of cells culture were stained with toluidine blue. Cells exposed to 1 µg/mL CYN. Detention of cellular growth and decrease of cell number caused by cellular death by apoptosis. Apoptotic bodies (arrows). Heterochromatin in apoptotic nucleus (arrowhead). Bar=20µm (**A, B**). Transmission electronic microscopy of SH-SY5Y cells exposed to 1 µg/mL CYN. Fractionated cytoplasm and formation of apoptotic bodies (arrows). Condensed chromatin in the inner face of the nucleolar membrane (asterisks). Fibrillar component of the nucleoulus (n). Nucleus (N). Bar=2µm (**C**). Semithin sections of cells culture were stained with toluidine blue. Cells exposed to 0.5 µg/mL CYN. No evidence of morphological alterations. Bar=20µm (**D**). Transmission electronic microscopy of SH-SY5Y cells exposed to 0.5 and 0.25 µg/mL CYN. Euchromatic nuclei with irregular shape (N). Cytoplasm with numerous free ribosomes (asterisk). Mitochondria (arrows). Bar=2µm (**E**).

Figure 14. Morphology of differentiated SH-SY5Y cells after 24 h of exposure to CYN. Phase-contrast microscopy of cells exposed to 0.3 µg/mL CYN. Rounded cells (arrows) with clear signs of cell death. Bar=100 µm (**A**). Semithin sections of cells culture were stained with toluidine blue. Cells exposed to 0.3 µg/mL CYN. Presence of numerous apoptotic bodies (arrows) as clear sign of cell death. Presence of dilated endoplasmic reticulum (arrowheads). Bar=25 µm (**B**). Transmission electronic microscopy of SH-SY5Y cells exposed to 0.3 µg/mL CYN. Condensed chromatin in the inner face of the nucleolar membrane (Chr). Bar=2µm (**C**). Phase-contrast microscopy of cells exposed to 0.15 µg/mL CYN. Rounded cells (arrows) with clear signs of cell death. Bar=100 µm (**D**). Semithin sections of cells culture were stained with toluidine blue. Cells exposed to 0.15 µg/mL CYN. Presence of dilated endoplasmic reticulum (arrowheads) and lipidic vacuoles (arrows). Bar=25 µm (**E**). Transmission electronic microscopy of SH-SY5Y

cells exposed to 0.15 µg/mL CYN. Condensed chromatin (Chr) in apoptotic nucleus (N). Bar=2µm (**F**). Semithin sections of cells culture were stained with toluidine blue. Cells exposed to 0.075 µg/mL CYN. Presence of numerous apoptotic bodies (arrows) as clear sign of cell death. Bar=25 µm (**G**). Transmission electronic microscopy of SH-SY5Y cells exposed to 0.075 µg/mL CYN. Euchromatic nuclei with irregular shape (N). Dilate endoplasmic reticulum (ER) and lipidic vacuoles (Lp). Bar=2 µm (**H**).

Figure 15. Morphology of undifferentiated SH-SY5Y cells after 24 h of exposure to MC-LR + CYN. Semithin sections of cells culture were stained with toluidine blue. Cells exposed to 37 µg/mL MC-LR + 1 µg/mL CYN. Intense cellular death by apoptosis. Heterochromatin accumulations in apoptotic nuclei (arrows). Cellular debris as apoptotic bodies (arrowheads). Bar=20µm (**A**). Transmission electronic microscopy of SH-SY5Y cells exposed to 37 µg/mL MC-LR + 1 µg/mL CYN. Heterochromatin condensation in the inner face of the nuclear membrane (asterisks). Nucleolar segregation with the fibrillary component (n). Apoptotic bodies formation (arrows). Autophagy vacuoles in the cytoplasm (arrowheads). Nucleus (N). Bar=2µm (**B**). Semithin sections of SH-SY5Y cells stained with toluidine blue. Cells exposed to 18.5 µg/mL MC-LR + 0.5 µg/mL CYN. Blister formation in cellular surface (arrows). Apoptotic bodies (arrowheads). Bar=20µm (**C, D**).

Figure 16. Morphology of differentiated SH-SY5Y cells after 24 h of exposure to MC-LR + CYN. Transmission electronic microscopy of SH-SY5Y cells exposed to 45 µg/mL MC-LR + 0.3 µg/mL CYN. Apoptotic nucleus (N) with heterochromatin condensation (Chr). Lipidic degeneration (Lp). Dilated endoplasmic reticulum (ER) with protein condensation (arrowheads). Pre-apoptotic bodies (arrows). Heterophagosome (Het). Nucleoulus (n) with the presence of a nuclear body (NB). Bar=2 µm (**A, B, C, D**). Semithin sections of cells culture were stained with toluidine blue. Cells exposed to 45 µg/mL MC-LR + 0.3 µg/mL CYN. Clear formation of apoptotic bodies (arrowheads). Bar=25 µm (**E**). Cells exposed to 22.5 µg/mL MC-LR + 0.15 µg/mL CYN and 11.25 µg/mL MC-LR + 0.075 µg/mL CYN. No significant alterations observed. Bar=25 µm (**F, G**).

Highlights

1. Microcystin-LR and cylindrospermopsin induced cytotoxicity in SH-SY5Y cells.
2. Both cyanotoxins presented an antagonistic effect when in combination.
3. The acetylcholinesterase activity vary with the exposure to the toxins.
4. Apoptosis was the main cell death mechanism observed by microscopy.

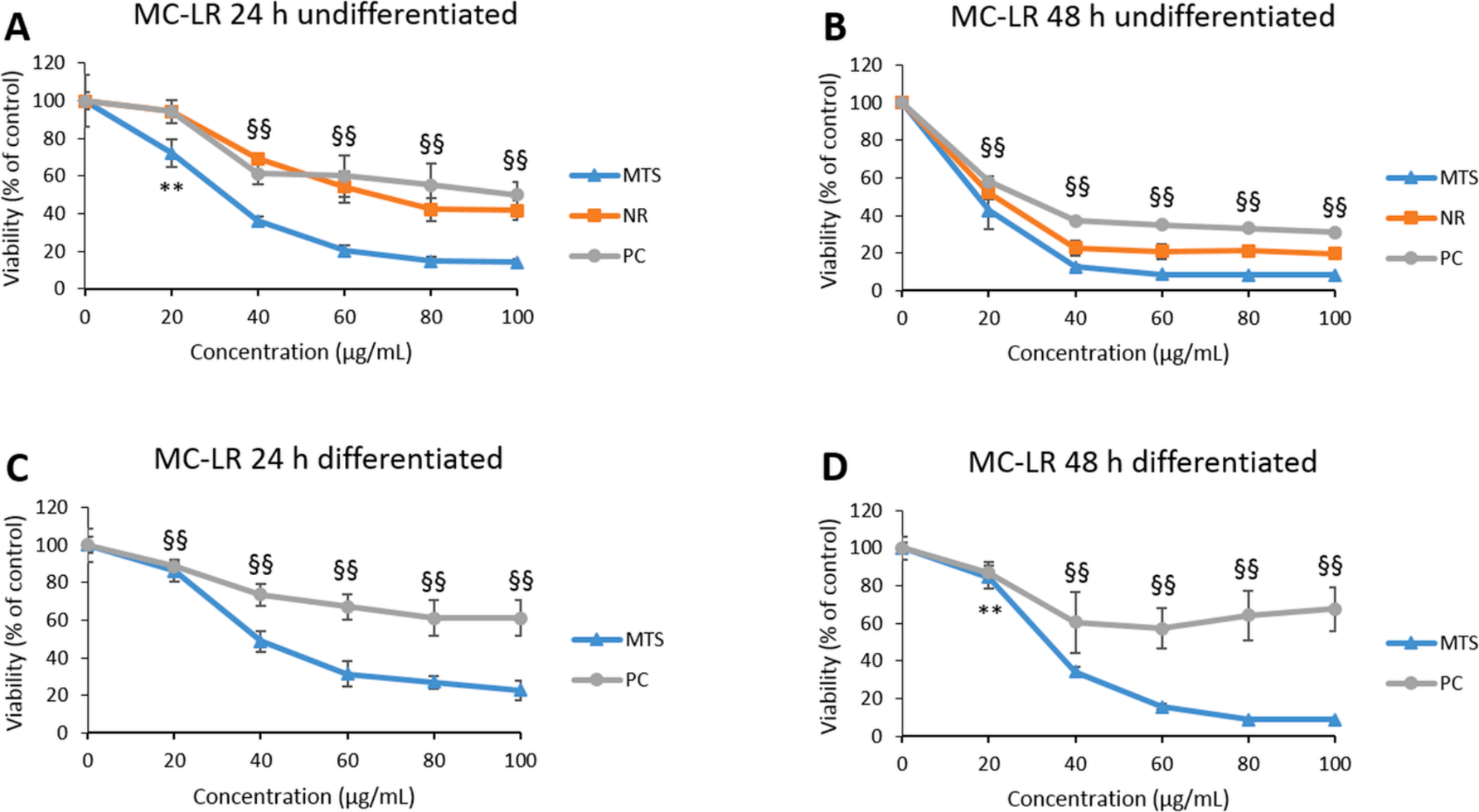
A
MC-LR 24 h undifferentiated
Viability (% of control)
Concentration (µg/mL)
MTS
NR
PC
**
§§
B
MC-LR 48 h undifferentiated
C
MC-LR 24 h differentiated
D
MC-LR 48 h differentiated

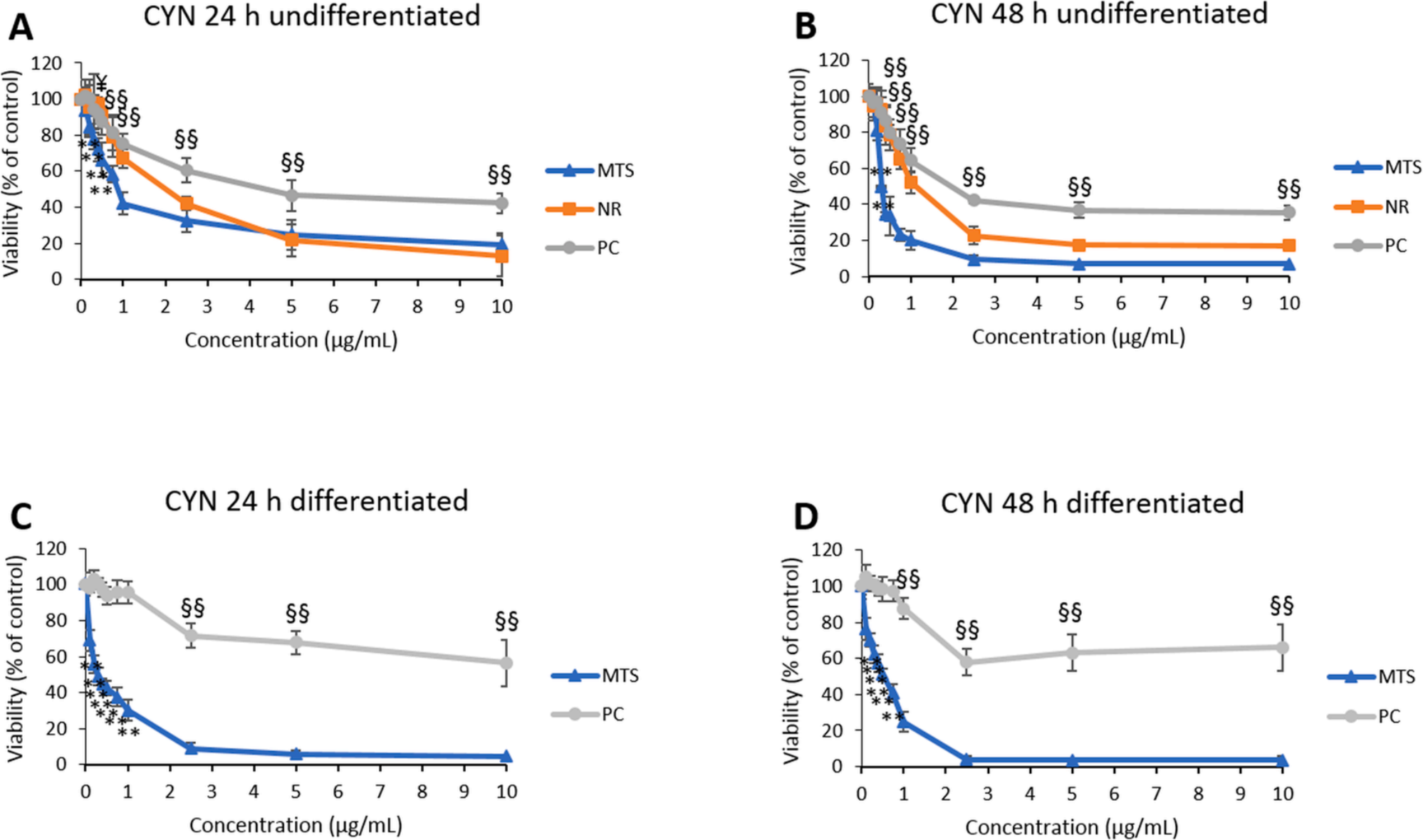
A
CYN 24 h undifferentiated
Viability (% of control)
Concentration (µg/mL)
MTS
NR
PC
B
CYN 48 h undifferentiated
Viability (% of control)
Concentration (µg/mL)
MTS
NR
PC
C
CYN 24 h differentiated
Viability (% of control)
Concentration (µg/mL)
MTS
PC
D
CYN 48 h differentiated
Viability (% of control)
Concentration (µg/mL)
MTS
PC

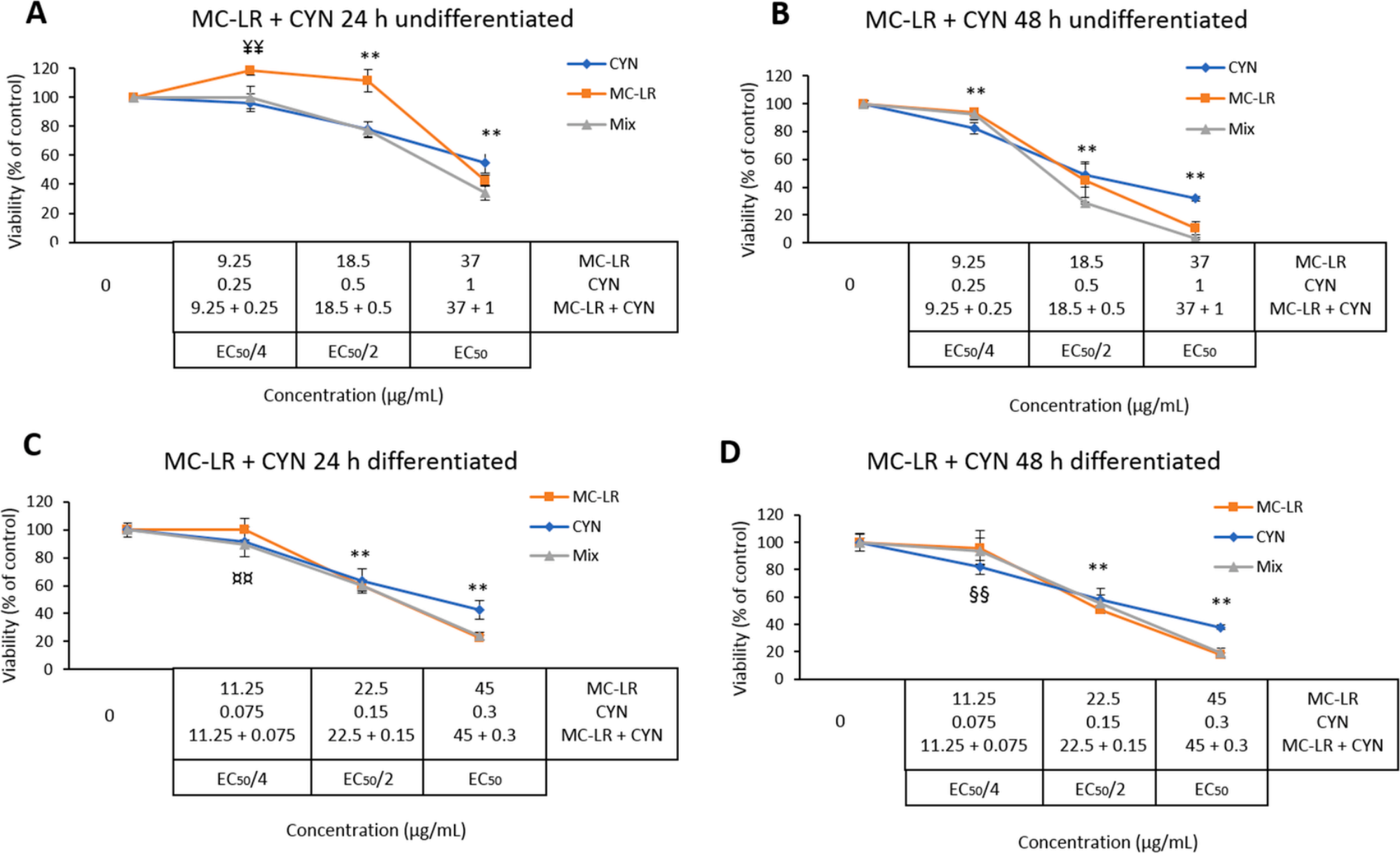
A
MC-LR + CYN 24 h undifferentiated
¥¥
**
**
CYN
MC-LR
Mix
Viability (% of control)
120
100
80
60
40
20
0
0
9.25
0.25
9.25 + 0.25
18.5
0.5
18.5 + 0.5
37
1
37 + 1
MC-LR
CYN
MC-LR + CYN
EC50/4
EC50/2
EC50
Concentration (µg/mL)
B
MC-LR + CYN 48 h undifferentiated
**
**
**
CYN
MC-LR
Mix
Viability (% of control)
120
100
80
60
40
20
0
0
9.25
0.25
9.25 + 0.25
18.5
0.5
18.5 + 0.5
37
1
37 + 1
MC-LR
CYN
MC-LR + CYN
EC50/4
EC50/2
EC50
Concentration (µg/mL)
C
MC-LR + CYN 24 h differentiated
¤¤
**
**
MC-LR
CYN
Mix
Viability (% of control)
120
100
80
60
40
20
0
0
11.25
0.075
11.25 + 0.075
22.5
0.15
22.5 + 0.15
45
0.3
45 + 0.3
MC-LR
CYN
MC-LR + CYN
EC50/4
EC50/2
EC50
Concentration (µg/mL)
D
MC-LR + CYN 48 h differentiated
§§
**
**
MC-LR
CYN
Mix
Viability (% of control)
120
100
80
60
40
20
0
0
11.25
0.075
11.25 + 0.075
22.5
0.15
22.5 + 0.15
45
0.3
45 + 0.3
MC-LR
CYN
MC-LR + CYN
EC50/4
EC50/2
EC50
Concentration (µg/mL)

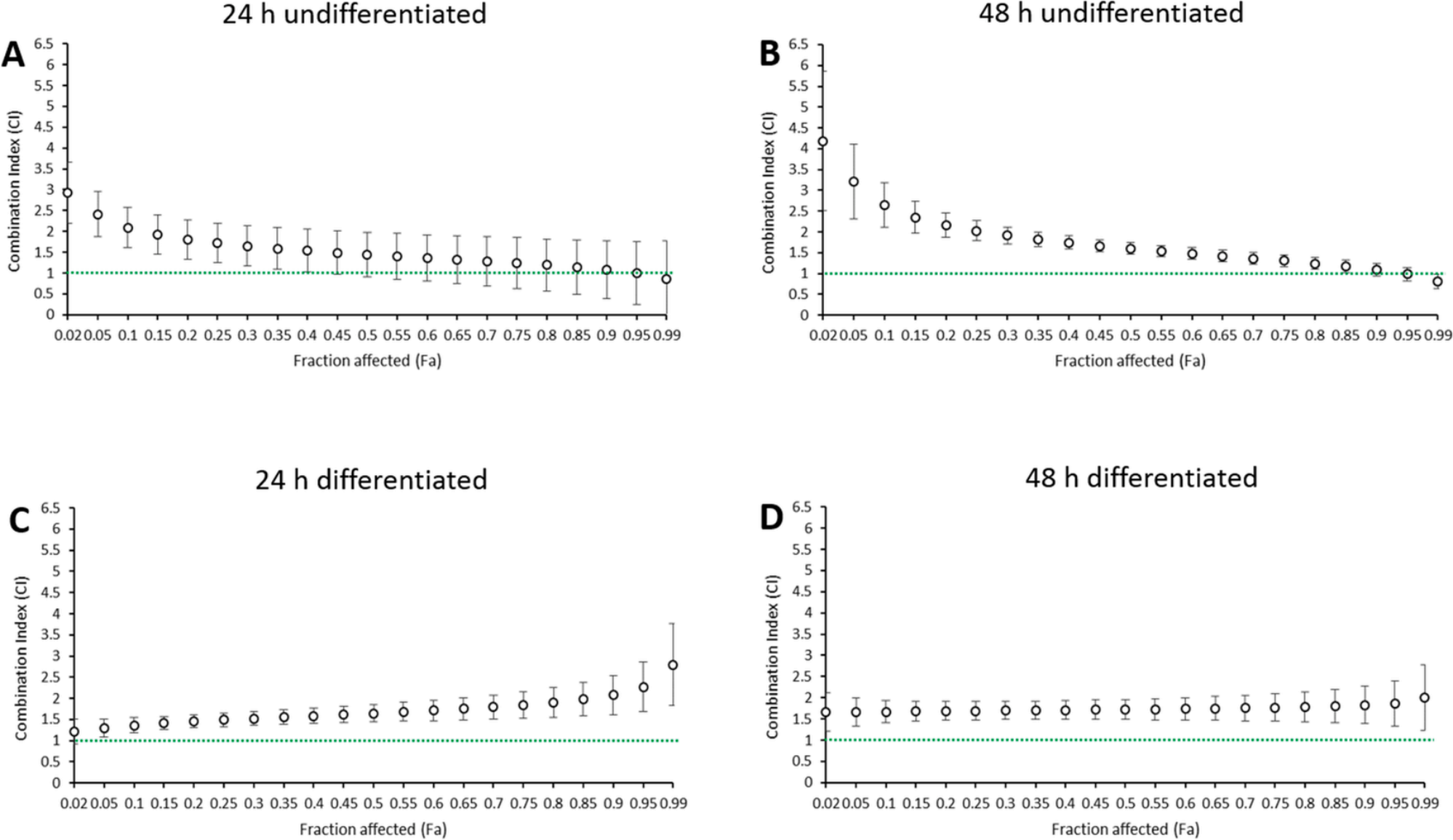
24 h undifferentiated
A
Combination Index (CI)
Fraction affected (Fa)
48 h undifferentiated
B
Combination Index (CI)
Fraction affected (Fa)
24 h differentiated
C
Combination Index (CI)
Fraction affected (Fa)
48 h differentiated
D
Combination Index (CI)
Fraction affected (Fa)

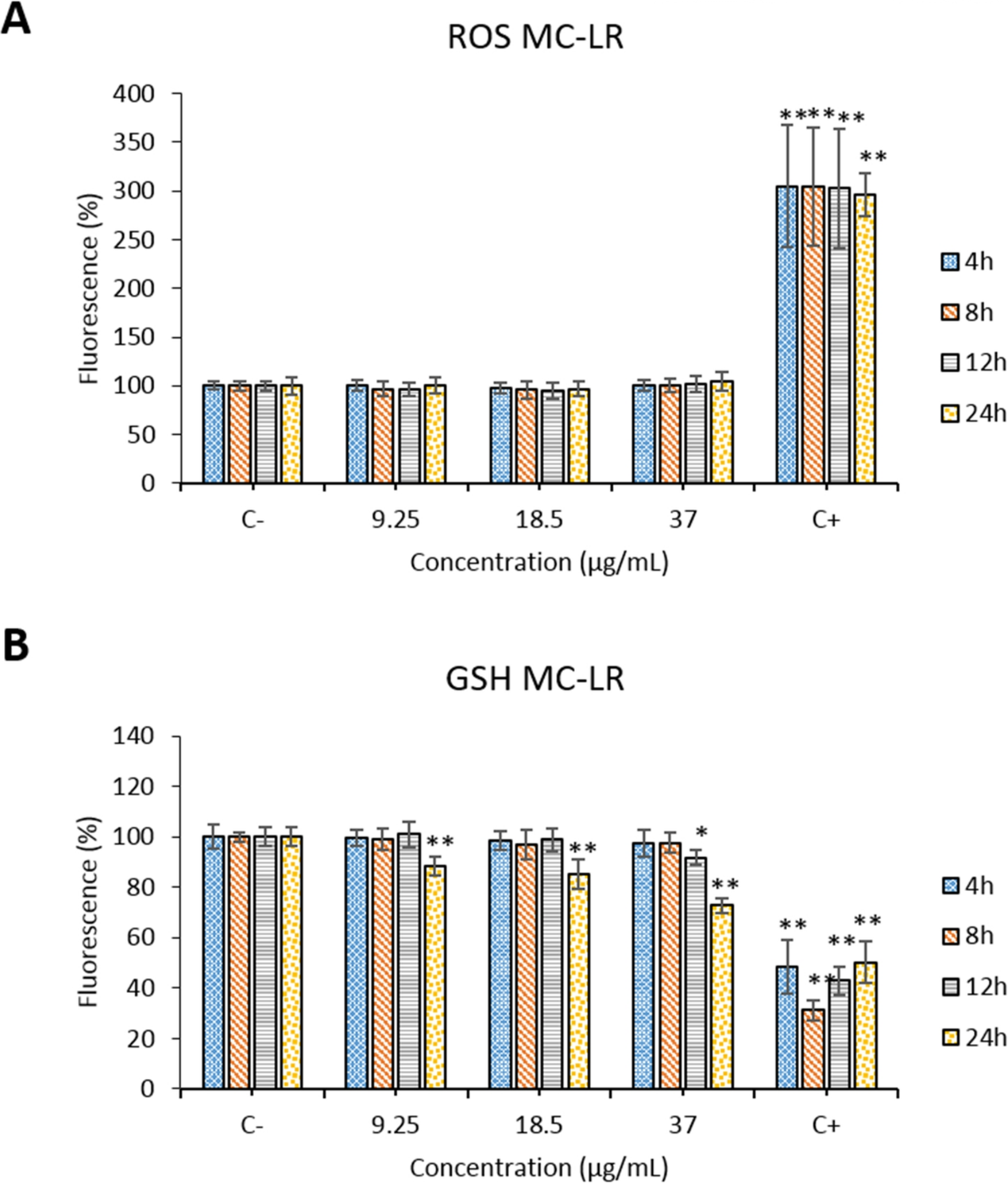
A
ROS MC-LR
Fluorescence (%)
400
350
300
250
200
150
100
50
0
C-
9.25
18.5
37
C+
Concentration (µg/mL)
4h
8h
12h
24h
B
GSH MC-LR
Fluorescence (%)
140
120
100
80
60
40
20
0
C-
9.25
18.5
37
C+
Concentration (µg/mL)
4h
8h
12h
24h

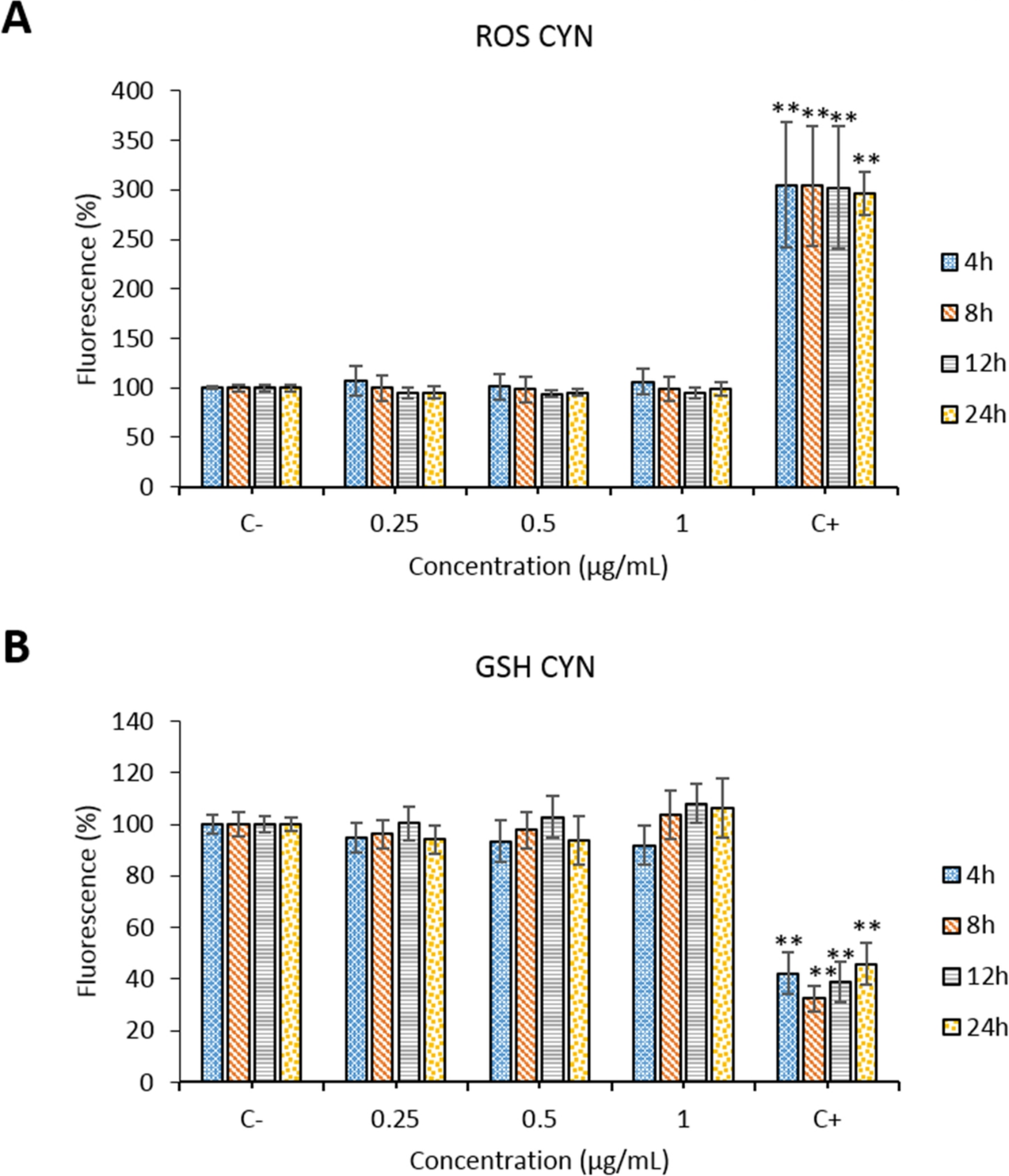
A
ROS CYN
Fluorescence (%)
400
350
300
250
200
150
100
50
0
C-
0.25
0.5
1
C+
Concentration (µg/mL)
4h
8h
12h
24h
B
GSH CYN
Fluorescence (%)
140
120
100
80
60
40
20
0
C-
0.25
0.5
1
C+
Concentration (µg/mL)
4h
8h
12h
24h

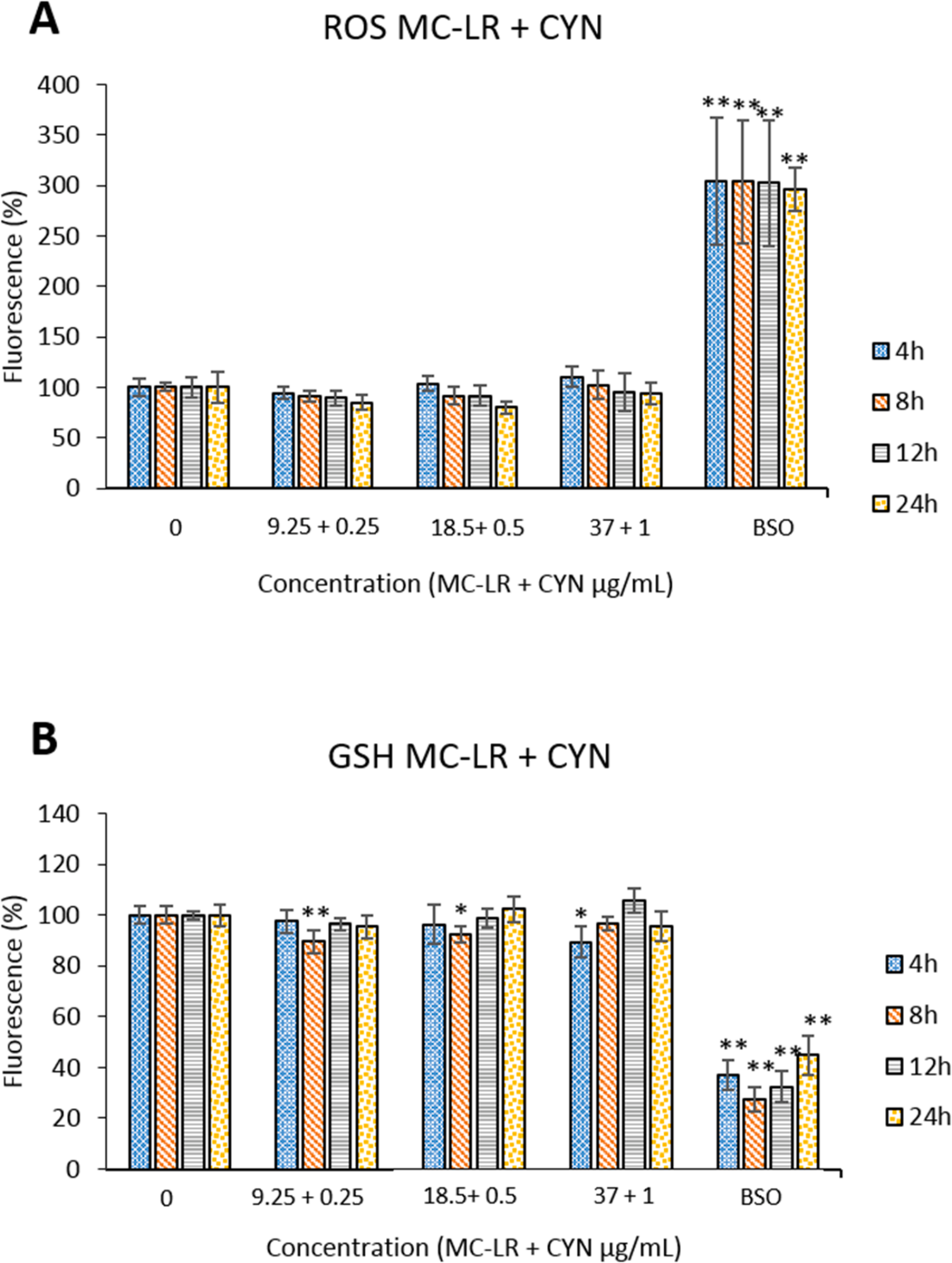
A
ROS MC-LR + CYN
Fluorescence (%)
400
350
300
250
200
150
100
50
0
0
9.25 + 0.25
18.5+ 0.5
37 + 1
BSO
Concentration (MC-LR + CYN µg/mL)
4h
8h
12h
24h
B
GSH MC-LR + CYN
Fluorescence (%)
140
120
100
80
60
40
20
0
0
9.25 + 0.25
18.5+ 0.5
37 + 1
BSO
Concentration (MC-LR + CYN µg/mL)
4h
8h
12h
24h

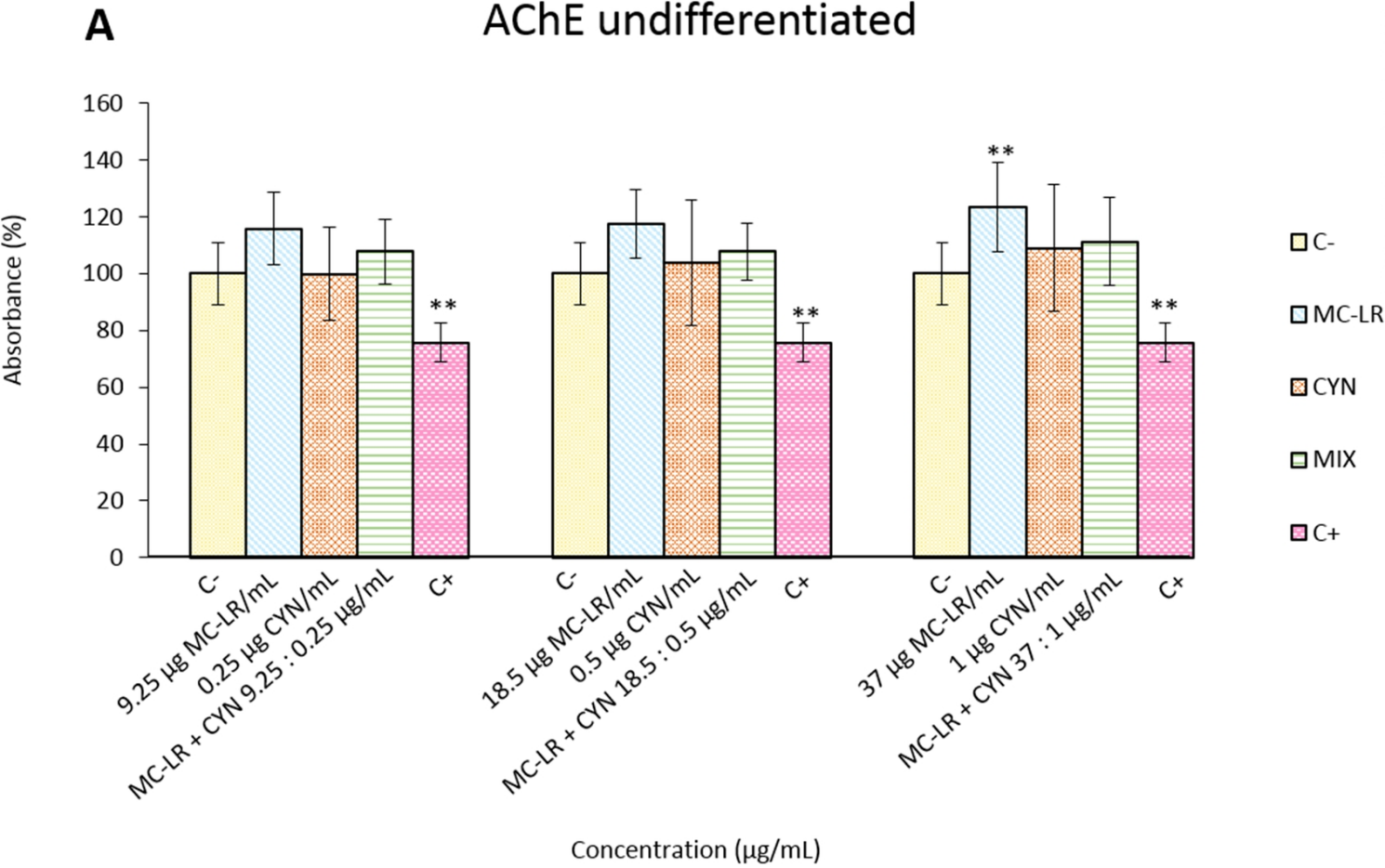
A
AChE undifferentiated
Absorbance (%)
160
140
120
100
80
60
40
20
0
**
**
**
**
**
C-
MC-LR
CYN
MIX
C+
C-
9.25 µg MC-LR/mL
0.25 µg CYN/mL
MC-LR + CYN 9.25 : 0.25 µg/mL
C+
C-
18.5 µg MC-LR/mL
0.5 µg CYN/mL
MC-LR + CYN 18.5 : 0.5 µg/mL
C+
C-
37 µg MC-LR/mL
1 µg CYN/mL
MC-LR + CYN 37 : 1 µg/mL
C+
Concentration (µg/mL)

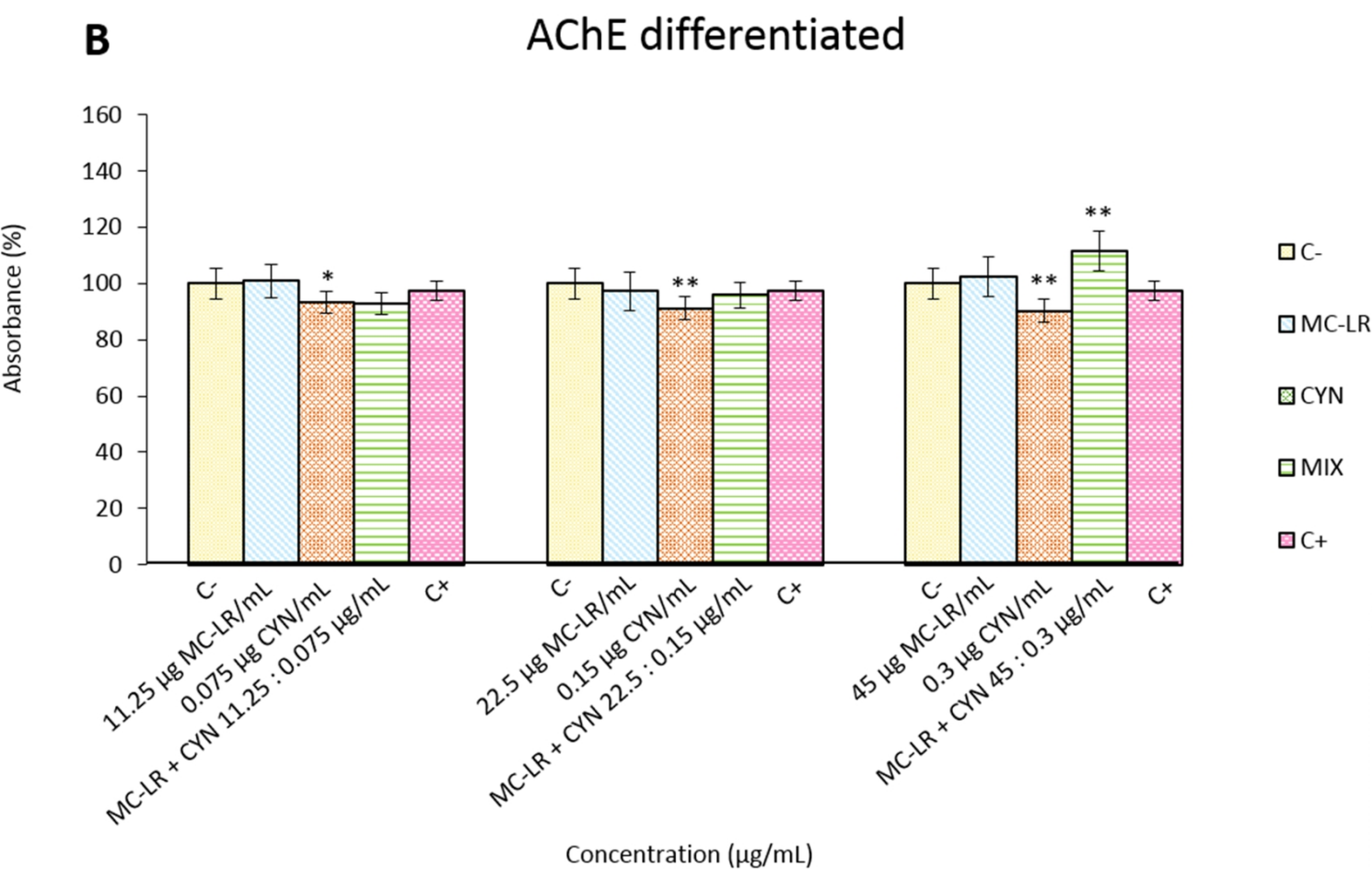
B
AChE differentiated
Absorbance (%)
160
140
120
100
80
60
40
20
0
*
**
**
**
C-
MC-LR
CYN
MIX
C+
C-
11.25 µg MC-LR/mL
0.075 µg CYN/mL
MC-LR + CYN 11.25 : 0.075 µg/mL
C+
C-
22.5 µg MC-LR/mL
0.15 µg CYN/mL
MC-LR + CYN 22.5 : 0.15 µg/mL
C+
C-
45 µg MC-LR/mL
0.3 µg CYN/mL
MC-LR + CYN 45 : 0.3 µg/mL
C+
Concentration (µg/mL)

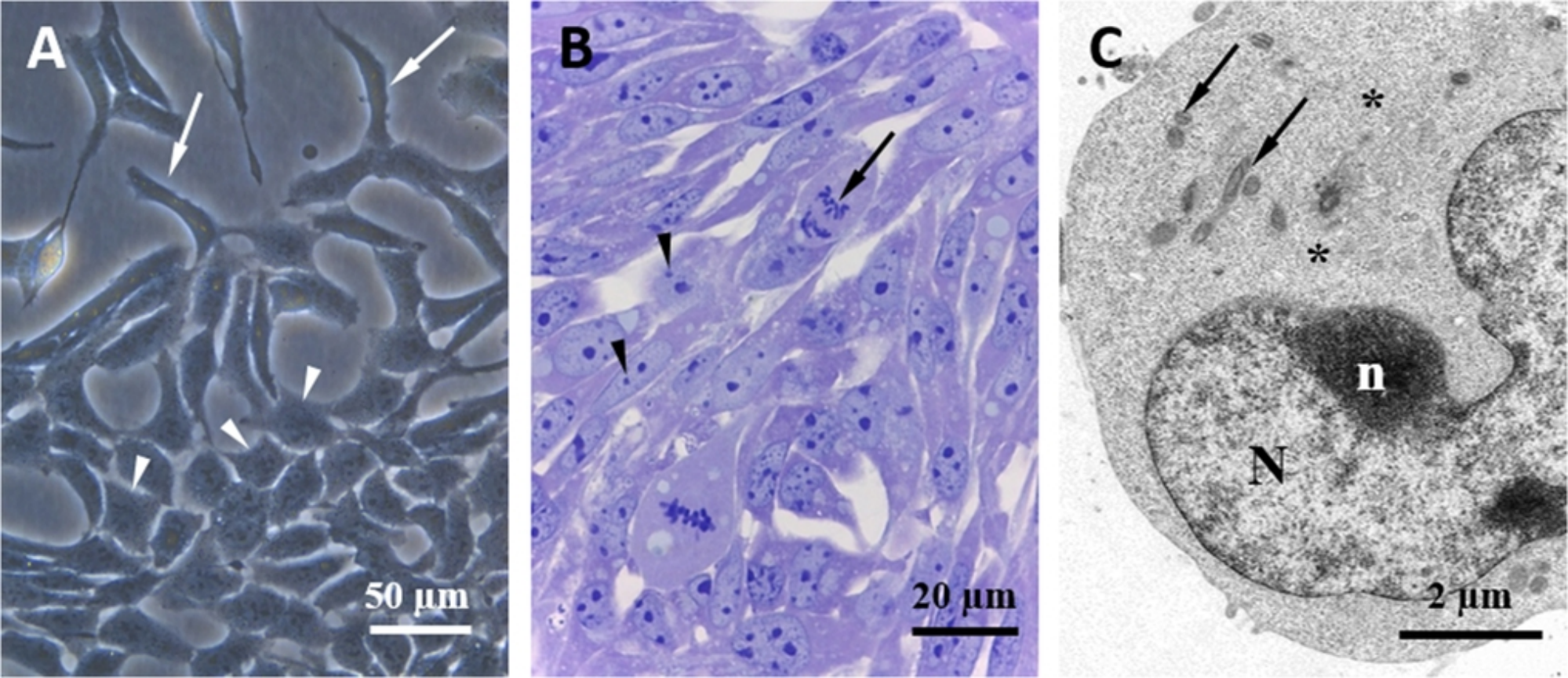
A
50 µm
B
20 µm
C
n
N
2 µm

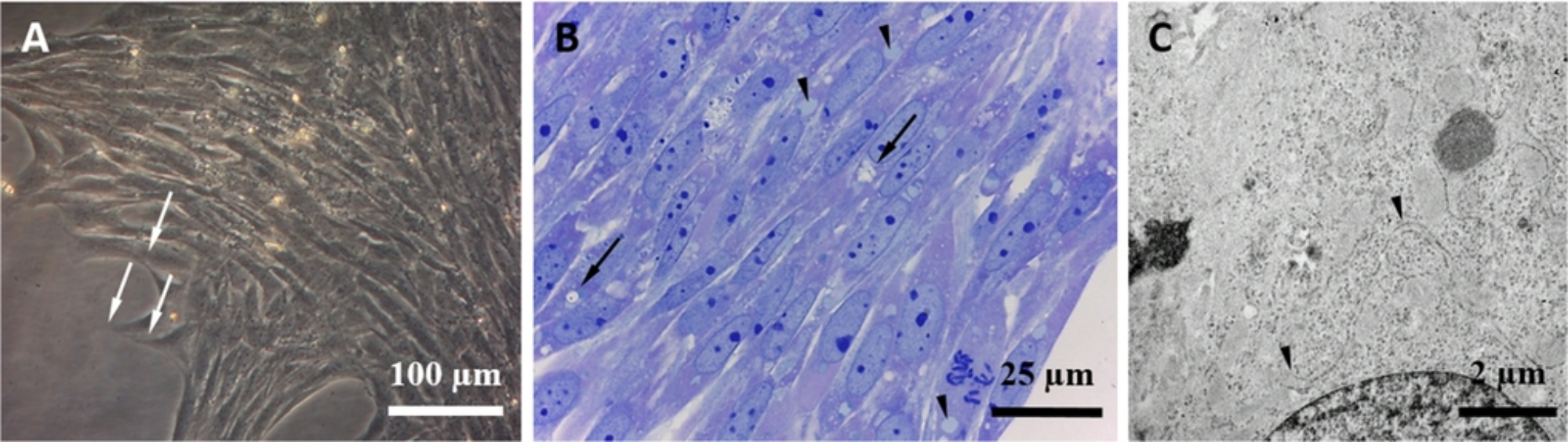
A
100 µm
B
25 µm
C
2 µm

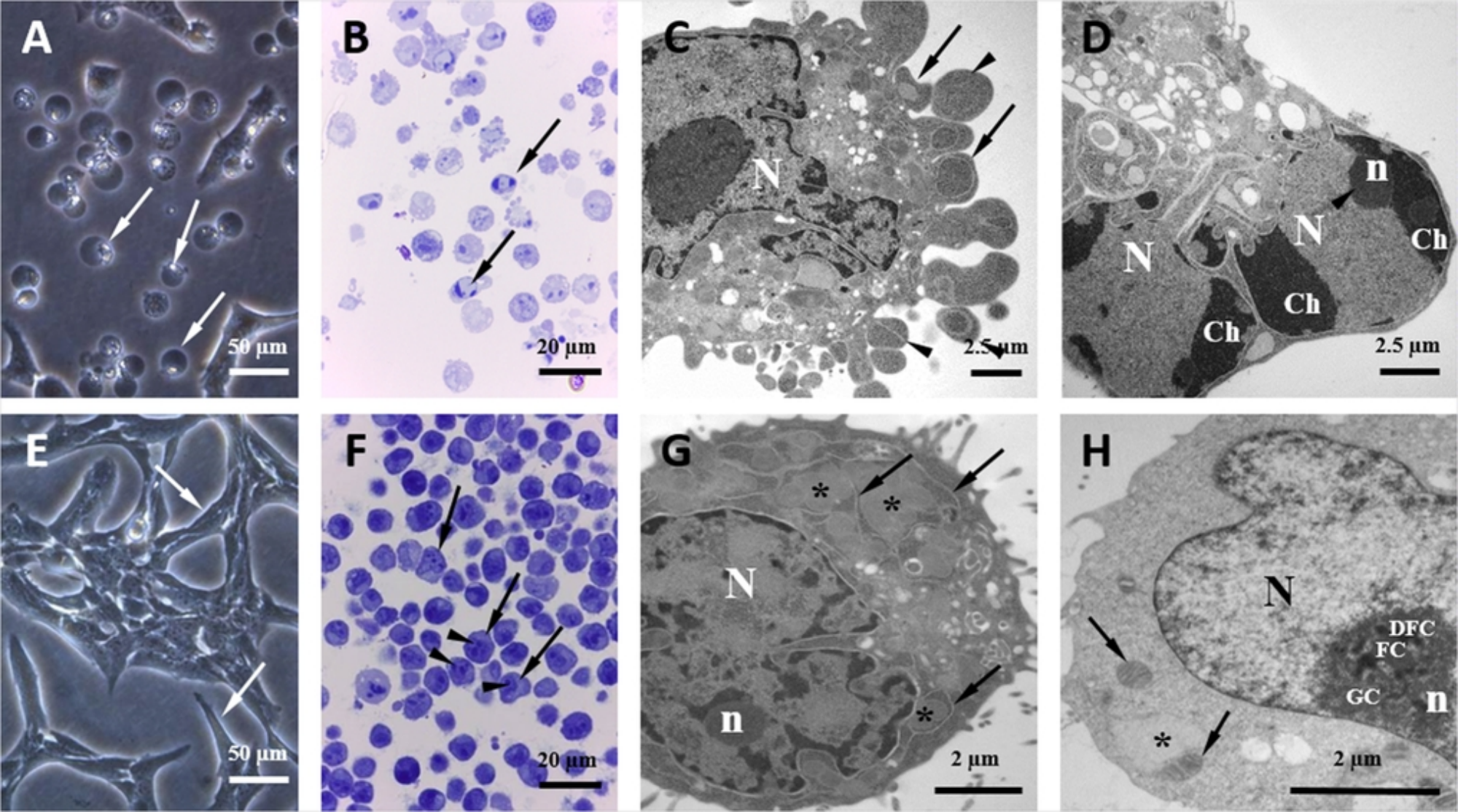
A
50 µm
B
20 µm
C
N
2.5 µm
D
n
N
N
Ch
Ch
Ch
2.5 µm
E
50 µm
F
20 µm
G
*
*
N
n
*
2 µm
H
N
DFC
FC
GC
n
*
2 µm

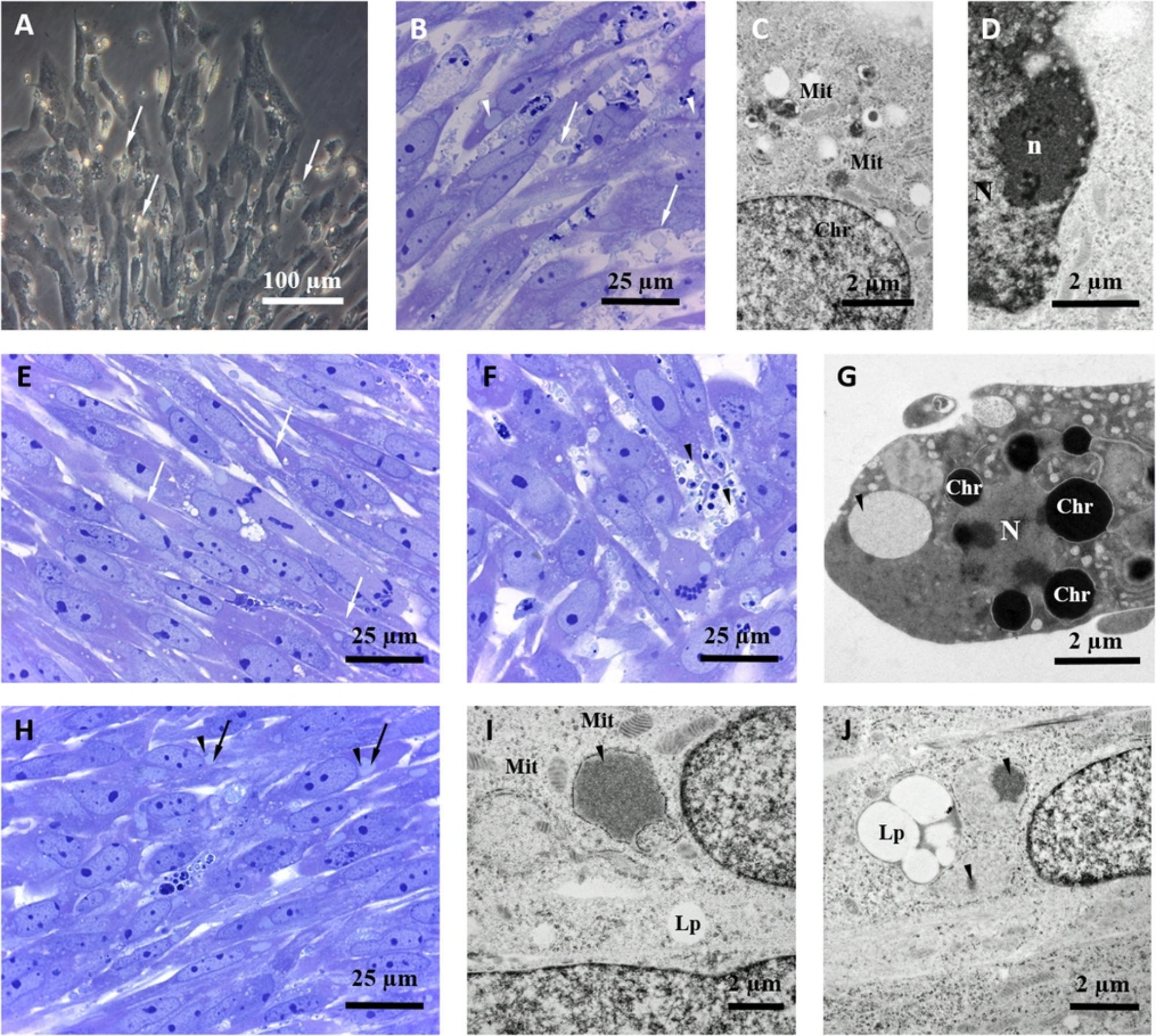
A
100 µm
B
25 µm
C
Mit
Mit
Chr
2 µm
D
n
N
2 µm
E
25 µm
F
25 µm
G
Chr
Chr
N
Chr
2 µm
H
25 µm
I
Mit
Mit
Lp
2 µm
J
Lp
2 µm

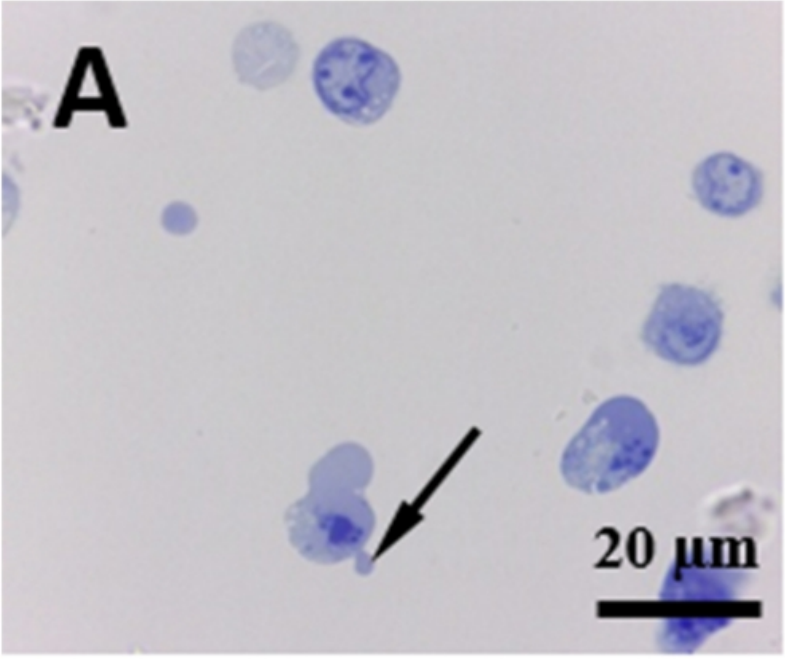
A
20 µm

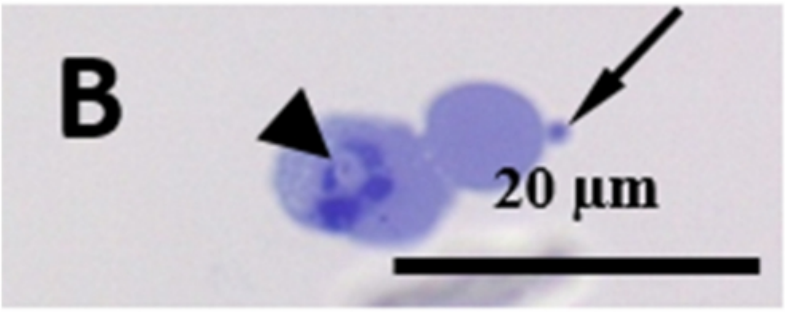
B
20 µm

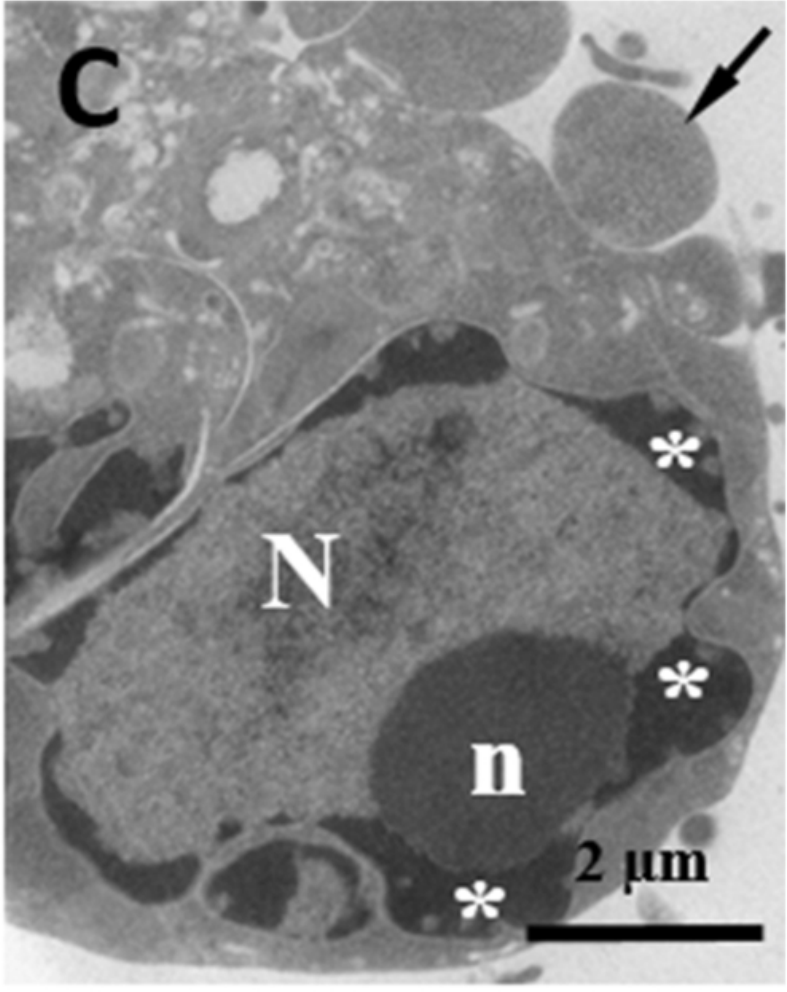
C
N
n
2 µm

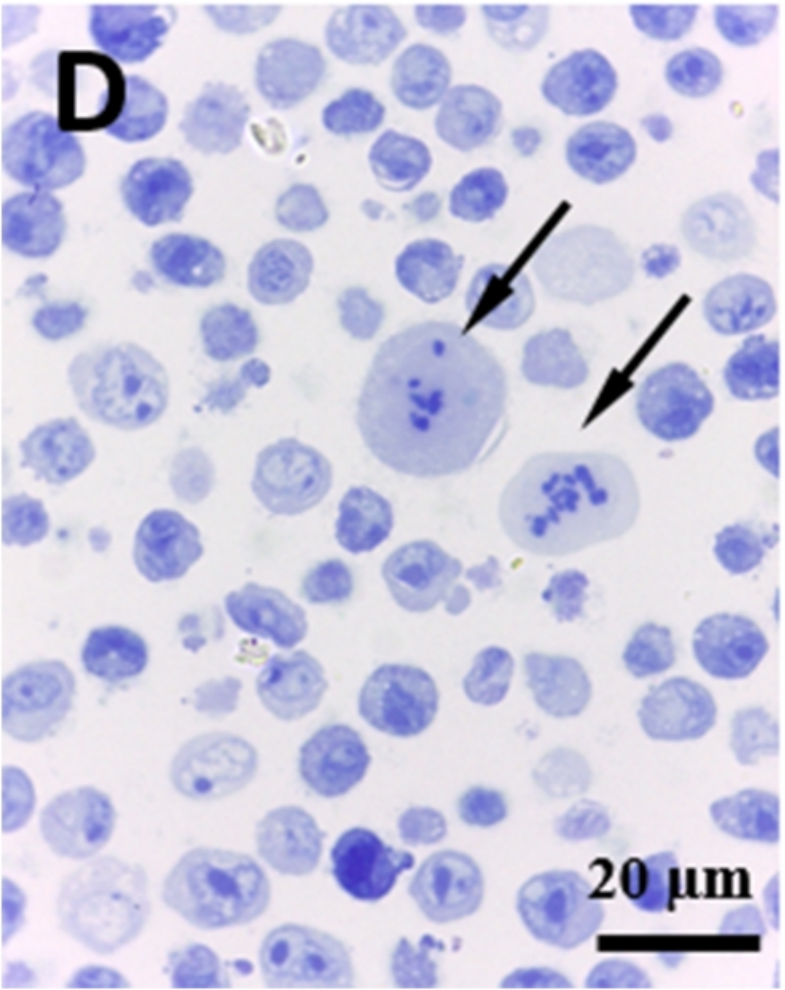
D
20 µm

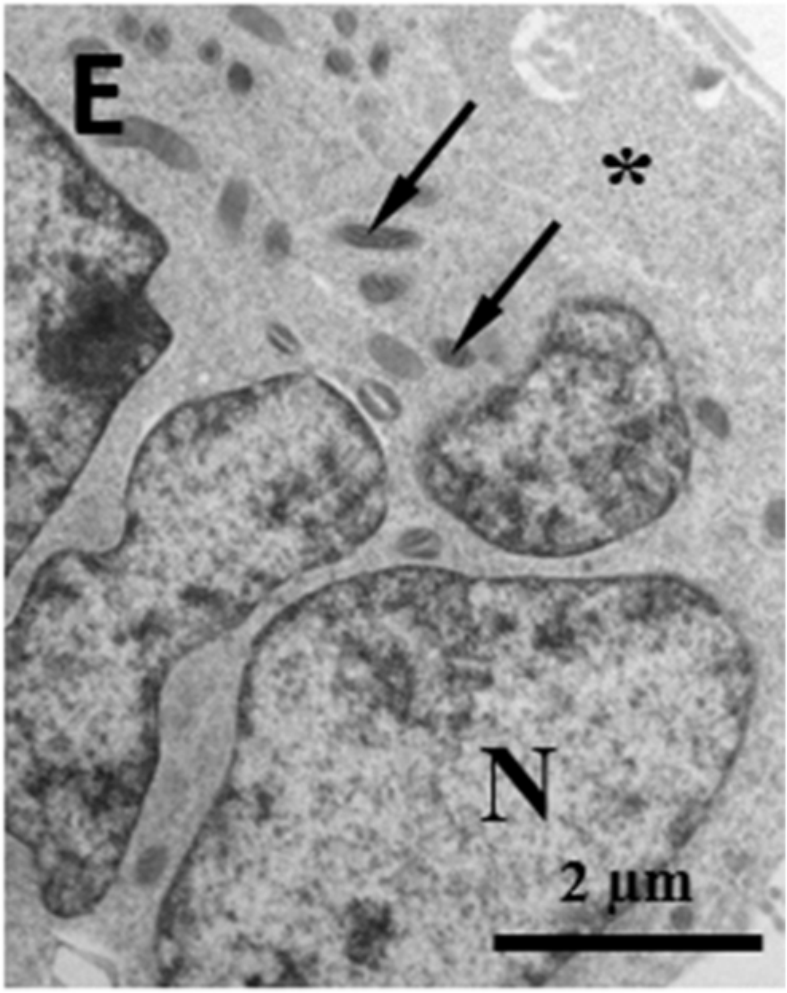
E
N
2 µm

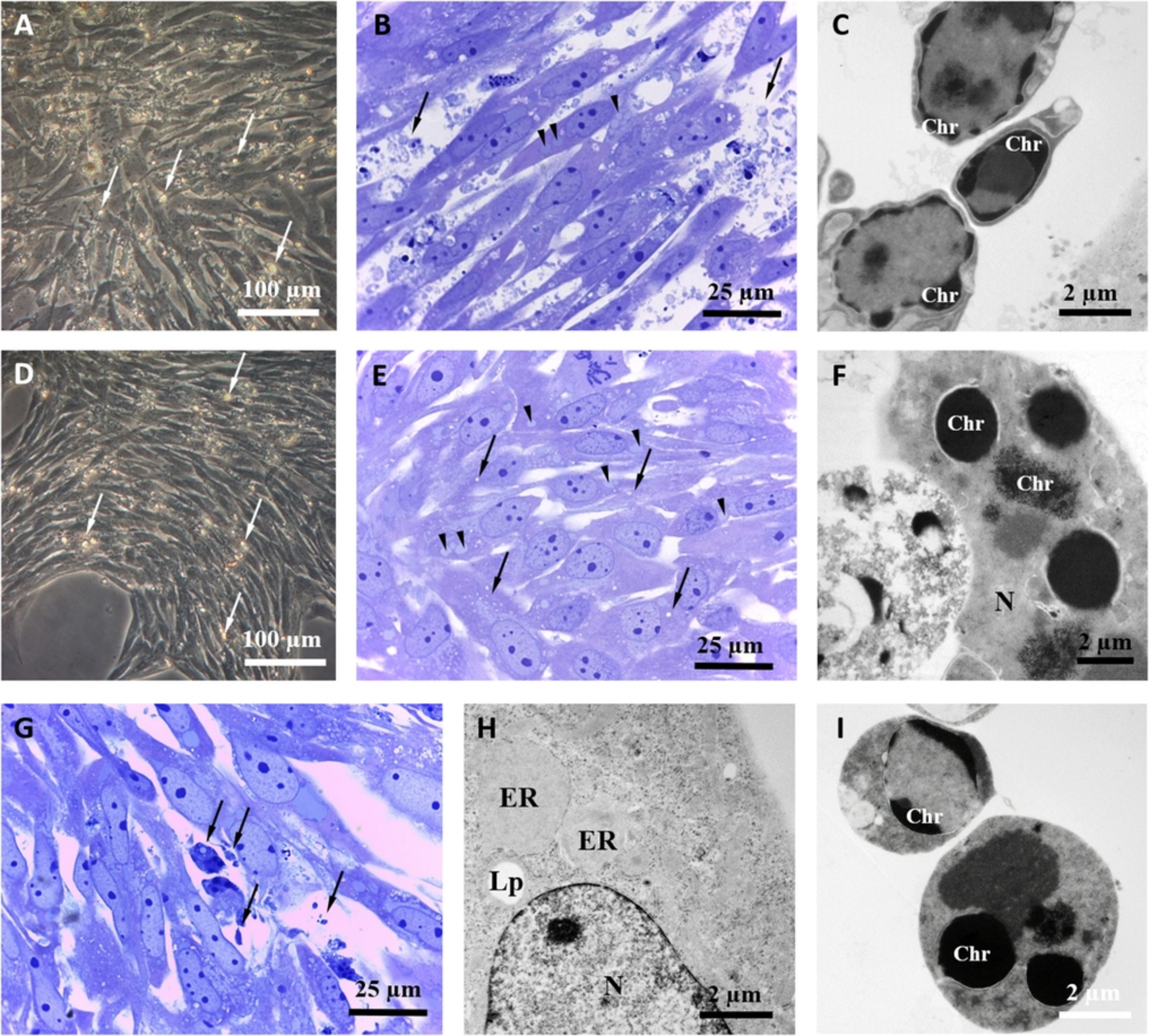
A
100 µm
B
25 µm
C
Chr
Chr
Chr
2 µm
D
100 µm
E
25 µm
F
Chr
Chr
N
2 µm
G
25 µm
H
ER
ER
Lp
N
2 µm
I
Chr
Chr
2 µm

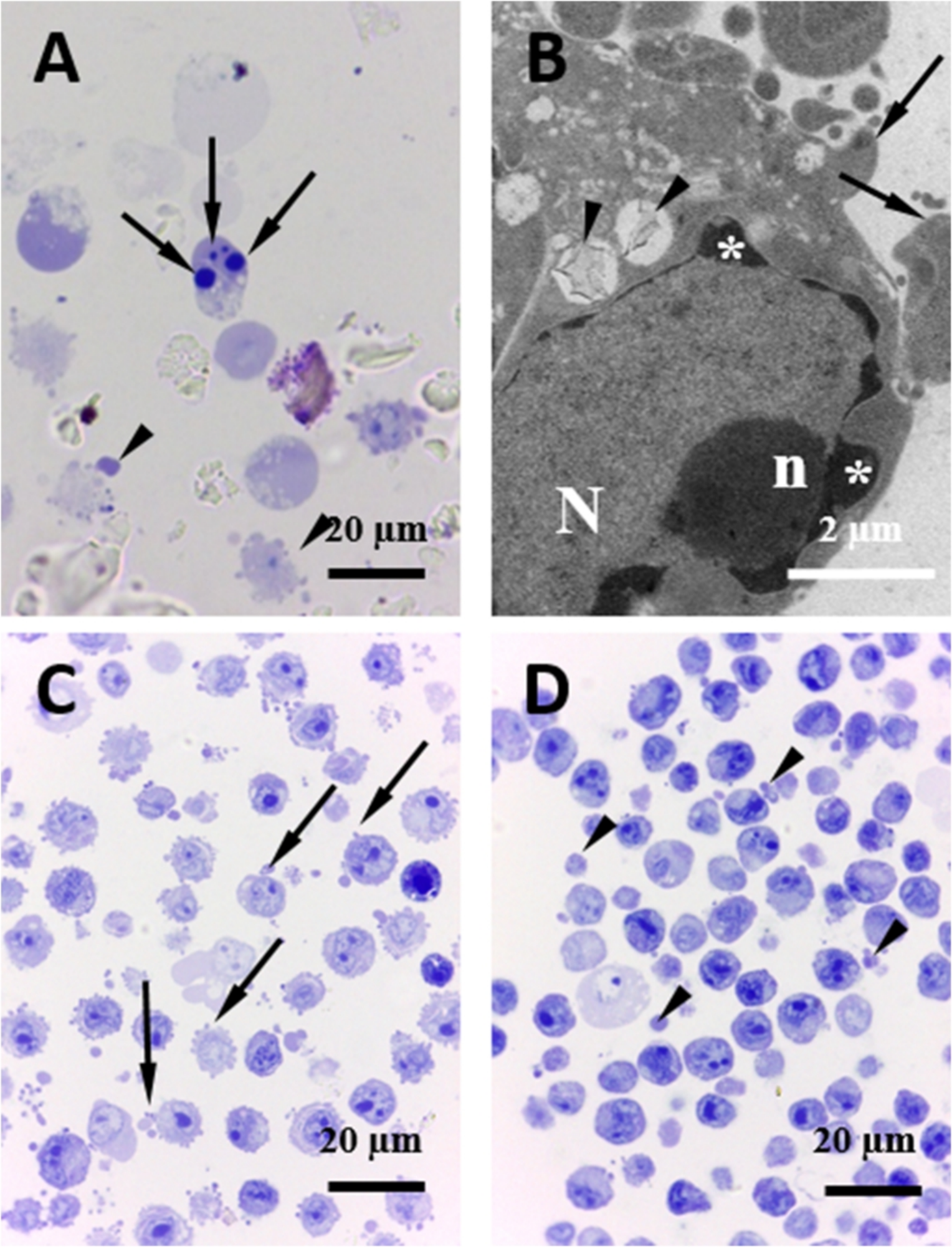
A
20 µm
B
*
N
n
*
2 µm
C
20 µm
D
20 µm

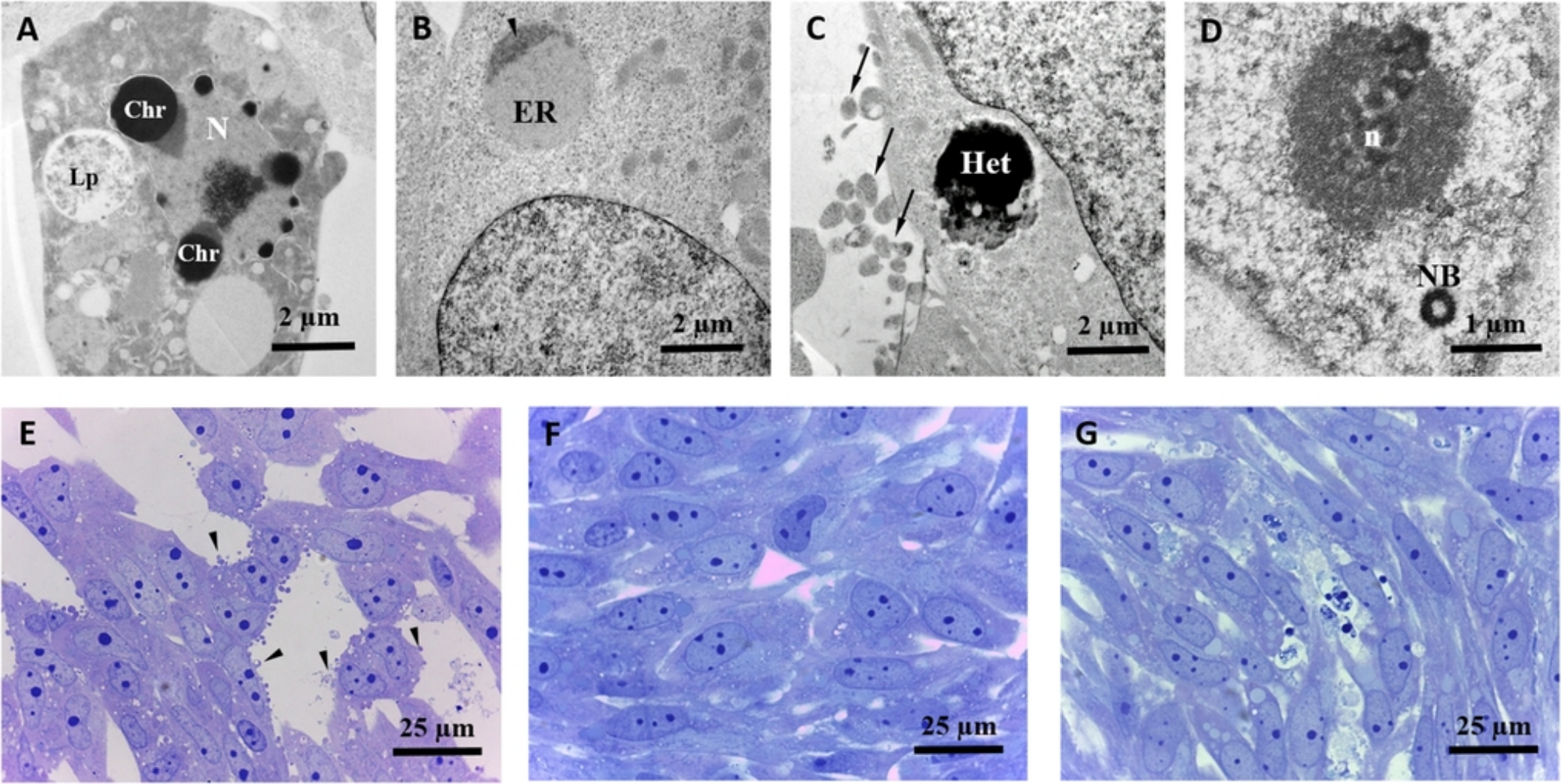
A
Chr
N
Lp
Chr
2 µm
B
ER
2 µm
C
Het
2 µm
D
n
NB
1 µm
E
25 µm
F
25 µm
G
25 µm

Toxin	Cell type	Time (h)	MTS assay		NR assay		PC assay	
			EC_{50} values (µg/mL)	Significant results (from) (µg/mL)	EC_{50} values (µg/mL)	Significant results (from) (µg/mL)	EC_{50} values (µg/mL)	Significant results (from) (µg/mL)
MC-LR	**Undifferentiated**	**24**	36.21 ± 1.89	20	67.69 ± 1.65	40	>100	40
		48	20.80 ± 2.08	20	24.27 ± 0.45	20	29.58 ± 2.70	20
	Differentiated	**24**	44.30 ± 0.91	20	-	-	>100	20
		48	37.01 ± 1.71	20	-	-	>100	40
CYN	**Undifferentiated**	**24**	0.87 ± 0.13	0.2	2.26 ± 0.29	0.5	4.37 ± 1.34	0.75
		48	0.32 ± 0.08	0.2	1.27 ± 0.27	0.4	2.01 ± 0.29	0.4
	Differentiated	**24**	0.30 ± 0.05	0.1	-	-	>10	2.5
		48	0.53 ± 0.02	0.1	-	-	>10	1

Table 1. Cytotoxicity results of undifferentiated and differentiated SH-SY5Y cells exposed to MC-LR and CYN. Results are expressed as mean ± s.d.

Cyanotoxin	Time (hours)	*Dm* (µg/mL)	*m*	*r*	CI values (undifferentiated cells)		
					CI_{50}	CI_{75}	CI_{90}
MC-LR	24	44.02	5.20	0.86603			
	48	19.13	3.51	0.99320			
CYN	24	1.01	2.20	0.98604			
	48	0.58	1.66	0.97832			
MC-LR + CYN	24	29.30	5.44	0.96064	1.45 Ant	1.24 Ant	1.08 Add
	48	16.17	4.25	0.99509	1.60 Ant	1.31 Ant	1.09 Add

Table 2. The parameter *m*, D_m and *r* are the antilog of x-intercept, the slope and the linear correlation coefficient of the median-effect plot, which signifies the shape of the dose-effect curve, the potency (IC_{50}), and the conformity of the data to the mass-action law, respectively. D_m and *m* values are used for calculating the CI value (CI< 1, indicates synergism (Syn); CI = 1, indicates additive effect (Add); CI > 1, indicates antagonism (Ant). IC_{50}, IC_{75} and IC_{90} are the doses required to inhibit proliferation 50, 75 and 90%, respectively. CalcuSyn software provide automatically the IC_{50}, IC_{75} and IC_{90} values.

Cyanotoxin	Time (hours)	*Dm* (µg/mL)	*m*	*r*	CI values (differentiated cells)		
					CI_{50}	CI_{75}	CI_{90}
MC-LR	24	30.17	4.14	0.96974			
	48	28.09	4.06	0.97042			
CYN	24	0.25	2.32	0.96974			
	48	0.23	2.53	0.96292			
MC-LR + CYN	24	27.32	2.37	0.99939	1.65 Ant	1.84 Ant	2.08 Ant
	48	26.50	3.00	0.99411	1.72 Ant	1.77 Ant	1.83 Ant

Table 3. The parameter *m*, D_m and *r* are the antilog of x-intercept, the slope and the linear correlation coefficient of the median-effect plot, which signifies the shape of the dose-effect curve, the potency (IC_{50}), and the conformity of the data to the mass-action law, respectively. D_m and *m* values are used for calculating the CI value (CI< 1, indicates synergism (Syn); CI = 1, indicates additive effect (Add); CI > 1, indicates antagonism (Ant). IC_{50}, IC_{75} and IC_{90} are the doses required to inhibit proliferation 50, 75 and 90%, respectively. CalcuSyn software provide automatically the IC_{50}, IC_{75} and IC_{90} values.